Published in final edited form as:
Dev Biol. 2025 April 01; 520: 155–170. doi:10.1016/j.ydbio.2025.01.005.

Epithelial and mesenchymal compartments of the developing bladder and urethra display spatially distinct gene expression patterns

Jasmine,
Divyeksha H. Baraiya,
T.T. Kavya,
Aparna Mandal,
Shreya Chakraborty,
Neha Sathish,
Cynthia Marian Rebecca Francis,
Diya Binoy Joseph*
Institute for Stem Cell Science and Regenerative Medicine (iBRIC-inStem), GKVK-Post, Bellary Road, , Bengaluru, Karnataka, 560065, India.

Abstract

The lower urinary tract is comprised of the bladder and urethra and develops from the cloaca, a transient endoderm-derived structure formed from the caudal hindgut. After cloacal septation to form the urogenital sinus and anorectal tract, the bladder gradually develops from the anterior portion of the urogenital sinus while the urethra elongates distally into the genital tubercle. The bladder is a target for regenerative and reconstructive therapies but engineering an impermeable bladder epithelial lining has proven challenging. Urethral epithelial function, including its role as an active immune barrier, is poorly studied and neglected in regenerative therapy. A deeper understanding of epithelial patterning of the urogenital sinus by the surrounding mesenchyme, also accounting for sex-specific differences, can inform regenerative therapies. In this study, we identified spatially distinct genes in the epithelial and mesenchymal compartments of the developing mouse bladder and urethra that could be potential drivers of patterning in the lower urinary tract. Our data revealed spatially restricted domains of transcription factor expression in the epithelium that corresponded with bladder or urethra-specific differentiation. Additionally, we identified the genes *Wnt2, Klf4* and *Pitx2* that localize to the mesenchyme of the developing bladder and could be potential drivers of bladder differentiation. Our data revealed an increase in

*Corresponding author. diyabj@instem.res.in (D. Binoy Joseph).

CRediT authorship contribution statement
Jasmine: Writing – original draft, Methodology, Investigation, Formal analysis, Data curation, Conceptualization. **Divyeksha H. Baraiya:** Investigation, Data curation. **Kavya T.T:** Investigation, Data curation. **Aparna Mandal:** Investigation. **Shreya Chakraborty:** Investigation. **Neha Sathish:** Investigation, Data curation. **Cynthia Marian Rebecca Francis:** Investigation. **Diya Binoy Joseph:** Writing – review & editing, Writing – original draft, Visualization, Methodology, Investigation, Funding acquisition, Formal analysis, Data curation.

Declaration of competing interest
None.

Europe PMC Funders Author Manuscripts

the expression of several chemokine genes including *Cx3cl1* and *Cxcl14* in the developing urethral epithelium that correlated with an increase in epithelial-associated macrophages in the urethra. A survey of sex-specific differences in epithelial and mesenchymal compartments revealed several differentially expressed genes between the male and female urethra but few sex-specific differences in bladder. By comparing spatially distinct gene expression in the developing lower urinary tract, our study provides insights into the divergent differentiation trajectories of the fetal bladder and urethra that establish their adult functions.

Keywords

Bladder; Urethra; Urogenital sinus; RNA-Sequencing; Transcription factors; Chemokines

1 Introduction

The epithelial linings of the bladder and urethra develop from the cloaca, a transient endoderm-derived structure located at the caudal portion of the hindgut (Georgas et al., 2015). In mice and humans, the cloaca undergoes septation to form separate genitourinary and anorectal tracts (Matsumaru et al., 2015; Xu et al., 2012). The ventral portion of the cloaca that contributes to the lower urinary tract is called the urogenital sinus, which serves as the precursor for bladder and urethra epithelium. Around embryonic day (E) 11 in the mouse, the bladder starts to emerge from the anterior portion of the urogenital sinus. The growth of the bladder epithelial lining is accompanied by an increase in proliferation and differentiation of the surrounding mesenchymal compartment (Georgas et al., 2015). Epithelial-mesenchymal interactions mediated by Shh signaling result in the formation of the bladder smooth muscle zone, separated from the epithelial layer by a non-smooth muscle mesenchymal layer called the lamina propria (Baskin et al., 2001; Cao et al., 2008, 2010). Studies in mice have uncovered several aspects of bladder development including the contribution of retinoid (Gandhi et al., 2013) and Shh signaling (Cheng et al., 2008) as well as the role of specific transcription factors like PPARG (Liu et al., 2019) and P63 (Karni-Schmidt et al., 2011).

While the anterior portion of the urogenital sinus differentiates into bladder, the posterior portion differentiates into the urethral lining. The urethral lining is a multi-layered stratified epithelium. Production of testosterone from fetal testis acts on the mesenchyme surrounding the urethra to induce specific signals that promote formation of prostate buds in males (Cunha et al., 2018). The distal urethra has been extensively studied as improper closure of the urethral tube can lead to the congenital defect hypospadia. Numerous genes and pathways including Hox transcription factors (Morgan et al., 2003; Tüzel et al., 2007), Shh (Perriton et al., 2002), Bmp, Wnt and Fgf signaling (Carmichael et al., 2013) have been implicated in normal urethral development with defects in these genes leading to hypospadias of varying degrees of severity. Similar to the distal end of other conduits like the vagina, anus and esophagus, the stratified epithelium of the urethra must withstand mechanical, chemical and pathogenic stress. In many epithelial tissues like skin, expression of antimicrobial peptides and innate defense proteins are intrinsically built into the epithelial

Europe PMC Funders Author Manuscripts

differentiation program (Elias, 2007). The role of the urethral lining in protecting against pathogens is understudied.

Most studies on development of the lower urinary tract have focused on three aspects: 1. bladder development and differentiation; 2. differentiation of external genitalia containing the distal portion of the urethral epithelium; and 3. the formation of prostate buds from the urethral epithelium. The development of bladder and urethra have been mostly studied in isolation, which has impeded a full understanding of the factors that drive bladder versus urethra fate. Epithelial-mesenchymal interactions play a critical role in tissue-specific differentiation. Fetal bladder mesenchyme can induce embryonic stem cells to express multiple markers of bladder differentiation (Oottamasathien et al., 2007). In an *in vivo* model of endoderm-specific *Dnmt1* deletion in mice, non-bladder epithelial cells migrating into the embryonic bladder acquired markers of bladder-specific differentiation (Joseph et al., 2018). This highlighted the capacity of embryonic bladder mesenchyme to induce bladder specific differentiation of non-bladder epithelium but the specific factors responsible for this reprogramming have not been identified. Factors directing bladder specific differentiation would be expected to have a spatially restricted pattern in the bladder mesenchyme. Comparison of epithelial and mesenchymal factors in bladder and urethra will result in the identification of specific genes that drive bladder- or urethra-specific differentiation.

A previous study carried out gene expression profiling using microarray technology on E13 and E14 mouse lower urinary tract and genital tubercle compartments to identify common and distinct gene sets (Chiu et al., 2010). In the current study, we used next generation sequencing techniques to compare the transcriptomic profiles of the epithelial and mesenchymal compartments of the bladder and proximal urethra at E16.5. E16.5 is a later stage of development than previously investigated (Chiu et al., 2010) at which time the bladder and urethra epithelium are distinct in terms of cellular markers and tissue architecture and start to resemble the adult epithelium. In this study, we describe novel gene markers that distinguish the developing bladder and urethral epithelium. Additionally, we describe epithelial and mesenchymal transcription factors that are spatially localized to either urethra or bladder. We found differential expression of genes involved in several developmental signaling pathways including Wnt, Bmp and Notch in the developing bladder and urethra. In keeping with the purported active barrier function of the urethra against pathogens, we identified increased expression of genes involved in barrier function, antimicrobial defense and immune regulation in the developing urethral epithelium. This correlated with the appearance of epithelial-associated macrophages in the fetal urethra which are absent from the bladder epithelium. Finally, we investigated sex-specific differences in epithelial and mesenchymal compartments of bladder and urethra. Our study revealed robust sex-specific differences in the epithelial and mesenchymal compartments of urethra with few sex-specific differences in either epithelial or mesenchymal compartments of bladder. This study provides a molecular comparison of gene expression patterns in the developing bladder and urethra providing intriguing insights into the patterning of the lower urinary tract.

2 Materials and methods

2.1 Animal husbandry and usage

Wildtype CD-1 mice (Charles River, USA # Crl:022) were obtained from the Animal Care and Resource Center at the Bangalore Life Sciences Cluster (BLiSC). All procedures on animals were approved by the inStem Institutional Animal Ethics Committee under protocol INS-IAE-2022/01(M2). Animals were housed in a specific pathogen free facility with routine health monitoring. Animals were provided ad-libitum chow (Safe-D131), autoclaved water and housed in individually ventilated cages. Mice were subjected to a 12-h light/dark cycle. Timed mating was performed with mice older than 7 weeks and noon of the day of vaginal plug detection was deemed to be embryonic day 0.5. For embryo collection, pregnant female mice at various stages of gestation were euthanized by approved methods and embryos were removed for fixation or RNA isolation. 8–10 week old CD-1 mice were used for adult stages.

2.2 Epithelial-mesenchymal separation

E14.5, E16.5 and E18.5 embryos were removed from timed pregnant females and the lower urinary tract comprising the bladder and proximal urethra were collected into ice-cold phosphate buffered saline (PBS). Epithelial-mesenchymal separation was performed as previously described (Joseph et al., 2018). Briefly, tissues were placed in sterile 1x Hank's Basic Salt Solution (HBSS) containing sodium bicarbonate (0.03%), antibiotic-antimycotic (Sigma Aldrich, A5955-20 ML) and 1% Trypsin w/v (Sigma Aldrich, T4799-5G). Tissues were incubated in the trypsin solution on ice at 4 C for 60 mins (E14.5 samples) or 90 mins (E16.5 and E18.5 samples). Tissues were washed in 1x HBSS containing sodium bicarbonate and antibiotic-antimycotic and briefly treated with DNase to remove excess genomic DNA from lysed cells. Tissues were then placed in cold 1x PBS and the urethra and bladder were separated with spring scissors. The epithelial and mesenchymal layers of the bladder and urethra of male and female embryos were mechanically separated with fine forceps and collected separately into RLT plus lysis buffer (Qiagen RNeasy Micro kit # 74004). Each E16.5 litter yielded 8 sample types: Male bladder mesenchyme, Male urethral mesenchyme, Female bladder mesenchyme, Female urethral mesenchyme, Male bladder epithelium, Male urethral epithelium, Female bladder epithelium and Female urethral epithelium. Only female samples were collected at E14.5 and E18.5 stages. Tissues from all male or female mice from a litter were pooled and a total of 3–4 biological replicates (from independent litters) for each sample type were collected. Tissue samples were lysed in RLT plus lysis buffer and homogenized using Qiashredder columns.RNA was isolated according to manufacturer instructions of the Qiagen RNeasy Micro kit.

2.3 RNA-sequencing

RNA-sequencing was performed on epithelial and mesenchymal samples from E14.5, E16.5 and E18.5 embryos to compare gene signatures in the urethra and bladder. For epithelial samples, 60 ng of total RNA was used for mRNA library prep while for mesenchymal samples 250 ng of total RNA was used. NEBNext Poly(A) mRNA Magnetic Isolation Module (#E7490L) was used for mRNA isolation according to manufacturer instructions. NEBNext® Ultra™ II Directional RNA Library Prep kit with Sample Purification Beads

(#E7765L) was used for library preparation according to manufacturer instructions. Samples were sequenced using NovaSeq 6000. 100 bp pair-ended reads were obtained. Basecalling and demultiplexing was performed using Illumina bcl2fastq. Read mapping was performed using hisat2 (Kim et al., 2019) using reference grcm38. Files in the .sam format obtained after read mapping were converted to unsorted.bam files using samtools (Li et al., 2009). Using samtools, .bam files were sorted and deduplicated. Feature counts were extracted from deduplicated.bam files using subread (Liao et al., 2013) with Gencode evidence-based annotation of the mouse genome (GRCm38), version M23 (Ensembl 98). Raw read counts were processed in R using DESeq2 (Love et al., 2014) to obtain normalized counts and differentially expressed genes. Genes with absolute fold change ≥0.5 and FDR (padj) < 0.01 were considered to be differentially expressed. Gene annotation was performed using DAVID (Sherman et al., 2022). Plots and heatmaps were generated using R packages DESeq2 and ggplot2 (Hadley, 2016). Gene subsets were generated using Venny (Oliveros, 2007). Gene set enrichment analysis was performed using ShinyGO 0.80 (Ge et al., 2020).

2.4 Histology and immunostaining

Whole embryos or dissected lower urinary tracts between E12.5-E18.5 were fixed in 4% paraformaldehyde in PBS or 10% Neutral buffered formalin overnight. Tissues were washed in 1x PBS and processed through a series of ethanol washes culminating in clearing with xylene before incubation in paraffin wax as previously described (Joseph et al., 2018, 2020). Tissue blocks were cut to obtain 5-μm sections on Superfrost plus charged slides. For immunostaining, sections were baked at 60 C, deparaffinized with xylene and rehydrated through a series of ethanol washes. Slides were washed in water and antigen retrieval was performed in a 0.01 M citric acid antigen retrieval solution by microwaving at high power for 20 min. Slides were blocked in blocking buffer (1x Tris-buffered Saline, 0.2 mM sodium azide, 0.1% (v/v) Tween-20, 0.1% (w/v) Bovine serum albumin Fraction V, 5% Horse serum) for 1 hr at room temperature. Primary antibodies diluted in blocking buffer were applied to the slides and incubated overnight at 4 C with gentle rocking. Slides were washed with 1x PBS and secondary antibodies were diluted in blocking buffer and incubated with tissue sections for 1 h at room temperature. Following washes, 300 nM of 4′,6-diamidino-2-phenylindole (DAPI) was applied to the slides for 5 min. After final washes with 1x PBS, slides were mounted in a glycerol based mounting media containing the antifade reagent n-propyl gallate. Primary and secondary antibodies used in this study are listed in Table S1. Hematoxylin-eosin labeling was performed on 5-μm paraffin sections following deparaffinization and rehydration. Slides were incubated with Gill's Hematoxylin No. 2 (Polysciences, 24243-500) for 1 min and a 0.25% eosin solution (Himedia Laboratories, GRM938) for 2 mins. Slides were mounted with Eukitt mounting media (Sigma Aldrich, 3989). Images were obtained using Zeiss Axio Observer 7.

2.5 In situ hybridization

In situ hybridization was performed as previously described (Abler et al., 2011; Guha et al., 2012; Tsao et al., 2009). For synthesis of Digoxigenin-11-UTP-Labeled riboprobes, cDNA from RNA isolated from embryonic mouse tissues was amplified with gene-specific primers to obtain T7 promoter tailed PCR products. PCR products were gel-purified and used as templates for in vitro transcription with T7 RNA polymerase and RNA labeling

mix containing DIG-UTP to generate RNA probes that will hybridize with mRNA targets as previously described (Abler et al., 2011). For *in situ* hybridization on paraffin sections, 5-μm sections were deparaffinized and rehydrated. All steps were carried out in DEPC treated water. Slides were heated in a microwave in Tris-based antigen retrieval buffer (Vector labs #H-3301-250). Following this, slides were washed and acetylation and permeabilization steps were carried out. Slides were incubated at room temperature in prehybridization buffer for 2 hrs (1x SSC, 50% formamide, 2% (v/v) Denhardt's reagent (Sigma Aldrich #D2532-5 ML), 5% (v/v) Salmon sperm DNA (Thermo Fisher #15-632-011)). Synthesized riboprobes were diluted in pre-hybridization buffer to a concentration of 2 ng/ul and incubated with sections overnight at 72 C in a hybridization oven. Slides were washed in 0.2x SSC buffer and blocked with 2% (v/v) sheep serum. Slides were incubated with 1:1000 Anti-Dig-AP antibody (Fab fragment, Sigma Aldrich #11093274910) overnight at 4 C. Following antibody incubation, slides were developed in BM-purple solution (Roche # 11442074001). After color development, sections were fixed in 4% PFA overnight, washed in 1x PBS and mounted with a glycerol based mounting solution. Images were obtained using Olympus IX73 microscope. The list of gene specific riboprobe primers is provided in Table S1.

2.6 RNAscope

RNAscope for detection of mRNA transcripts was performed using RNAScope 2.5 Hd Reagent Kit Brown (ACD #322371) following manufacturer instructions. Tissues were fixed for 16–24 h depending on size in 10% neutral buffered formalin at room temperature. 5-micron paraffin sections were probed with RNAscope® Probe-Mm-*Wnt2* (ACD #313601) or Probe-Mm-*Cx3cl1* (ACD #426211). Standard pretreatment steps were performed with 15 min of antigen retrieval by steaming and 30 min of protease treatment. After development of the stain, tissues were counterstained with hematoxylin and mounted. Images were obtained using Olympus IX73 microscope. mRNA molecules were approximated as single dots of brown staining from the RNAscope assay. ImageJ Cell counter plugin was used to quantify the number of dots per 100 μm^2 area of tissue. Bartlett's test was performed to test equality of variance between the two groups. Unpaired, two-tailed *t*-test was performed assuming unequal variance (Welch's *t*-test). Null hypothesis was rejected when p-value <0.05.

2.7 Quantitative reverse transcriptase PCR

qRT-PCR was performed on bladder and urethra epithelial and mesenchymal tissues samples obtained from E14.5 and E16.5 embryos. RNA was converted to cDNA using iScript™ Reverse Transcription Supermix for RT-qPCR (Biorad # 1708841). Quantitative PCR was carried out using QuantStudio 5 with PowerUp SYBR Green Mastermix for qPCR (Applied Biosystems # A25742) or Maxima SYBR Green qPCR Master Mix (2X) (Thermo Scientific, K0253) and gene specific primers. Statistical analysis was performed with R statistics software. All analyses were performed on log2 fold change values. Bartlett's test was performed to test equality of variance between the two groups. Unpaired, two-tailed student's t-test was performed with significance level cut-off of 0.05 to reject null hypothesis. Primer sequences are provided in Table S1.

2.8 Single cell RNA-sequencing data analysis

A published dataset (Qiu et al., 2024) was used to assess single nuclei RNA-sequencing of E16.0-E16.75 whole mouse embryos. Run 26 from GSE228590, which includes samples from E16.0-E16.75, was used. Cells annotated as “Epithelial_cells” under major_trajectory were sub-setted and re-clustered using Seurat 4.3.0 (Satija et al., 2015). Feature plots for marker genes were generated in Seurat using the FeaturePlot function. Custom gene modules with urethral and bladder epithelial markers were created and scoring was done using AddModuleScore function in Seurat. Scores were visualized in Feature plots.

2.9 Data sharing

Sequence data have been deposited in NCBI GEO under accession numbers GSE253102, GSE253103, GSE275615 and GSE275616.

Information on materials and reagents used in this study are provided in the Key Resources Table in the supplementary information (Table S1).

3 Results

3.1 The urethra and bladder epithelium show temporal differences in differentiation

The urogenital sinus differentiates into the bladder anteriorly and the urethra posteriorly. To assess epithelial differentiation in the developing lower urinary tract across stages, we performed immunostaining with antibodies to epithelial proteins Keratin 5 (KRT5), SOX2 and Uroplakin 1a (UPK1A). In the adult lower urinary tract, KRT5 marks the basal epithelial layer of bladder and urethra (Georgas et al., 2015). SOX2 expression has previously been described in urethra and prostate (McAuley et al., 2019). In the developing mouse bladder, uroplakin expression is observed in I (intermediate) and S (superficial cells) (Gandhi et al., 2013). In the adult, uroplakin expression marks the bladder urothelial boundary and is enriched in adult mouse bladder superficial cells, although lower expression is observed in other cell layers of the mouse bladder (Georgas et al., 2015; Yu et al., 2019). We observed that SOX2 marks the developing urethra from E12.5 but is absent in the bladder at all stages (Figure S1 A-H). KRT5 expression is first detected at E15.5 (Figure S1 D) in the urethra and coincides with the rapid increase in cell layers of urethral epithelium. A gradual increase in KRT5 expression is observed in the bladder starting from E16.5 onwards (Figure S1 F). UPK1A expression is present in the bladder dome region at a low level at E14.5 (Figure S1 C). Gradually, the expression extends towards the bladder neck and also to a small extent on the dorsal side of the urethra (Figure S1 D). While the epithelial lining of the urethra continued to add cell layers, the bladder lining went from smooth to folded between E16.5 and E17.5 (Figure S1 A-H). The folded nature of the bladder lining at E17.5 resembles that of the adult bladder epithelium (Georgas et al., 2015).

We then labeled lower urinary tract sections from different stages of development with antibodies to KRT5, PPARG and Keratin 4 (KRT4) (Figure S1 I-P). PPARG is a transcription factor expressed in the bladder epithelium that regulates expression of Uroplakin genes (Liu et al., 2019). A few PPARG + cells are found in the bladder lining within the dome region at E12.5 (Figure S1 I). Expression of PPARG in the bladder

gradually increases over the course of development. The appearance of PPARG expression at E12.5 precedes the expression of UPK1A in the bladder lining at E14.5 (Figure S1 C). Notably, PPARG is expressed in a small patch on the dorsal urethra (Figure S1 L) that also expresses UPK1A (Figure S1 D). From E12.5-E16.5, PPARG is expressed across multiple cell layers of the bladder lining (Figure S1 I-L, N) but is gradually confined to the apical UPK1A + cell layer at E17.5 (Figure S1 P). Mirroring the apical expression of PPARG and UPK1A in the bladder epithelium, KRT4 is expressed in a 1–2 cell thickness in the apical layer of the urethral lining from E15.5-E17.5 (Figure S1 L, M, O).

Overall, differentiation of urethra and bladder epithelium from the urogenital sinus occurs gradually over the course of development with significant divergence in expression of cellular markers resembling the adult epithelial linings occurring between E16.5 and E17.5.

3.2 The epithelial compartments of the developing bladder and urethra have spatially distinct gene expression patterns

To assess transcriptomic differences between the developing bladder and urethra, we isolated epithelium from E16.5 bladder and urethra (Fig. 1 A, Figure S2) and performed bulk RNA-sequencing. Separation of the epithelium and mesenchyme was verified by performing qPCR for the mesenchymal gene Vimentin (*Vim*) and the epithelial genes E-cadherin (*Cdh1*) and Uroplakin 1a (*Upk1a*). *Vim* was enriched in the mesenchymal compartments while *Cdh1* and *Upk1a* were enriched in the epithelial compartments of the bladder and urethra (Figure S3 A-C). Principle component analysis showed that bladder and urethra epithelial samples segregated by tissue type and sex (Fig. 1 B). Assessment of differentially expressed genes in the bladder and urethra epithelial compartments revealed 3042 genes upregulated in the bladder epithelium and 3394 genes upregulated in the urethral epithelium with an absolute log2 fold change of ≥0.5 and adjusted p-value of ≤0.01 (Fig. 1C–Tables S2–S3). We generated a heatmap of known bladder and urethra-specific genes and novel markers identified in this analysis. In keeping with the highly stratified nature of the urethral lining, the epithelial compartment of the urethra expressed several Keratin genes including *Krt4, Krt13, Krt14* and *Krt17*. The bladder lining displayed a different keratin profile where *Krt7* and *Krt20* were predominantly expressed. As expected, the bladder lining showed higher expression of Uroplakin genes *Upk1a, Upk2* and *Upk3a* along with previously described bladder expressed genes (Liu et al., 2019) like *Pparg, Fabp4* and *Sprr1a* (Fig. 1 D).

We identified two novel markers specific to the urethral epithelium BCL2 and ARG1. BCL2, an anti-apoptotic protein (Opferman and Kothari, 2018), was expressed exclusively in all cell layers of the urethral epithelium and absent in the bladder lining (Fig. 1E–H, Figure S4 A-D). ARG1 or Arginase-1 was detected in the apical layer of the urethral epithelium starting from E14.5. ARG1 expression increased at E16.5 but was still limited to the apical layer of the urethral epithelium (Fig. 1I–L, Figure S4 E-H). We identified LGALS3 or Galectin-3, a beta-galactosidase binding lectin protein (Liu et al., 1995) as an early marker of bladder epithelium. LGALS3 was expressed in the bladder of E12.5 and E14.5 embryos and was absent from the urethral epithelium at these stages. At E16.5, LGALS3 was expressed in the intermediate and apical layers of the bladder epithelium and showed correlation with UPK1A expression, while limited expression was observed in

the urethral epithelium, with LGALS3 expressing cells confined to the apical layer of the urethral epithelium (Fig. 1M–P, Figure S4 I-L). Additionally, we identified *Wnt6* and *Lgr5* as markers of urethral epithelium and *Aqp3* as a marker for bladder epithelium and verified the differential expression of these markers by qPCR at an earlier developmental stage, E14.5 (Fig. 1Q–S).

We performed an unbiased analysis for KEGG pathway enrichment in the bladder and urethra compartments. The results indicate the enrichment of various metabolic pathways in the bladder epithelium including Fatty acid metabolism, oxidative phosphorylation, PPAR signaling pathway. Additionally, pathways like Drug metabolismcytochrome P450, Glutathione metabolism, Metabolism of xenobiotics by P450, Chemical carcinogenesis-reactive oxygen species were enriched in the bladder epithelium (Fig. 1T–Tables S4–S5).

In the urethral epithelium, we observed enrichment of several developmentally relevant signaling pathways including Wnt, Notch, Hippo and TGF-beta. Additionally, pathways regulating pluripotency of stem cells and transcriptional mis-regulation in cancer, MAPK and PI3K-Akt pathways were also enriched in urethral epithelium (Fig. 1U–Tables S6–S7). We assessed differences in growth factor gene expression in the urethra and bladder epithelium. We observed increased expression of the Fgf ligands *Fgf1, Fgf9* and *Fgf11* and the receptor *Fgfr2* in urethral epithelium compared to bladder epithelium. In particular, *Fgf9* expression was highest in female urethral epithelium (Figure S5 A). Notch signaling is a key developmental signaling pathway (Siebel and Lendahl, 2017). We observed higher expression of three Notch receptors *Notch1, Notch2* and *Notch3* in urethral epithelium compared to bladder epithelium. Expression of the Notch ligand *Jag2* and Notch regulator gene *Hes6* (Bae et al., 2000) was also increased in urethral epithelium (Figure S5 B). From the transcriptomic data, we observed spatial segregation of Wnt pathway genes in the urethra and bladder epithelium. The Wnt ligands *Wnt3, Wnt3a, Wnt6* and *Wnt10b* showed higher expression in the urethral epithelium whereas *Wnt11* expression was higher in the bladder epithelium. Wnt receptors *Fzd3* and *Fzd6*, along with co-receptors *Lrp5* and *Lrp6* displayed higher expression in the urethral epithelium while *Fzd5* showed increased expression in the bladder epithelium (Figure S5 C).

3.3 The bladder and urethral epithelium display spatially restricted expression of transcription factors

Restricted domains of transcription factor expression can pattern developing tissues (Danopoulos et al., 2018). To identify transcription factors that are exclusively expressed in the developing urethra or bladder epithelium, we curated a heatmap of developmentally relevant genes across transcription factor families (Fig. 2 A). We observed increased expression of *Sox2* and *Sox9* in urethral epithelium compared to bladder epithelium. *Sox2* (McAuley et al., 2019) and *Sox9* (Schneider et al., 2019) have been previously described for their roles in prostate. At E16.5, we found that *Gata3* expression is increased in the urethral epithelium compared to the bladder epithelium. Assessment of GATA3 protein by immunostaining showed nuclear GATA3 expression across the urethra and bladder epithelium at E12.5 and E14.5 (Fig. 2B–C). At E16.5, nuclear GATA3 is present in in

the basal and supra-basal layers of the urethral epithelium while present mostly in the apical layer of bladder epithelium (Fig. 2D–E, Figure S6 A-D).

We identified GATA2 as a transcription factor with higher expression in bladder epithelium compared to urethral epithelium at E16.5 (Fig. 2 A). We assessed protein expression of GATA2 across E12.5, E14.5 and E16.5. At E12.5 and E14.5, expression of nuclear GATA2 was higher in bladder epithelium compared to urethral epithelium (Fig. 2F–G). In E16.5 embryos, nuclear GATA2 is highly expressed in the apical layer of bladder epithelium and nuclear protein levels are reduced in urethral epithelium (Fig. 2H–I, Figure S6 E-H). The apical layer of urethral epithelium is completely devoid of detectable GATA2 expression while the dorsal patch of the urogenital sinus epithelium that expresses UPK1A (Figure S1 D) and PPARG (Figure S1 L) had higher levels of nuclear GATA2 (Fig. 2 H).

Further, we validated expression of three urethra-specific transcription factors *Irx1, Irx2* and *Pax9* identified from our transcriptomic data (Fig. 2 A) in E14.5 embryos (Fig. 2J–L). *Irx1* expression has been previously described in the urethral epithelium (Amato and Yao, 2021). We identified *Irx2* and *Pax9* as novel urethral epithelial-specific transcription factors in the lower urinary tract showing differential expression at E14.5 and E16.5.

3.4 Bladder and urethral epithelial gene signatures are conserved across developmental time

To identify differentially expressed genes in the bladder and urethra at an earlier and later embryonic stage than E16.5, we performed microdissection of E14.5 and E18.5 bladder and urethral epithelia. Differential expression analysis was performed to identify bladder and urethra specific epithelial genes at these stages (Figure S7 A-B, Figure S8 A-B, Tables S8–S9). A core group of differentiation markers *Krt14, Krt17, Bcl2, Arg1, Wnt6, Fzd10* and *Lgr5* show higher expression in the urethral epithelium compared to the bladder epithelium at E14.5, E16.5 and E18.5 (Fig. 1 D, Figure S7 C, Figure S8 C). *Krt7, Sprr1a, Fabp4, Pparg, Upk1a, Upk2, Upk3a* and *Aqp3* form a core group of marker genes that show higher expression in the bladder epithelium compared to the urethral epithelium at E14.5, E16.5 and E18.5 (Fig. 1 D, Figure S7 C, Figure S8 C). The transcription factors *Gata2* and *Pparg* show higher expression in the bladder epithelium at E14.5 and the differential expression is maintained at E16.5 and E18.5. In the urethra, several transcription factors including *Sox2, Sox9, Pax9, Irx1, Irx2* begin to be differentially expressed at E14.5 and are maintained at higher levels in the urethral epithelium at E16.5 and E18.5 (Fig. 2 A, Figure S7 D, Figure S8 D). This demonstrates that bladder and urethral epithelial identities are established as early as E14.5.

We performed gene ontology analysis to identify enrichment of KEGG pathways in differential expressed genes across developmental time. We studied three categories of differential expressed genes in the bladder and urethral epithelial compartments: 1. Shared (common at E14.5, E16.5 and E18.5) 2. Early/Mid (common to E14.5 and E16.5 only) and 3. Mid/late (common to E16.5 and E18.5 only). Strikingly, similar pathways were enriched for Shared and Early/Mid categories. In the bladder, metabolic pathways were enriched within both these categories while a different set of pathways were enriched in the Mid/Late category including ECM-receptor interaction, relaxin signaling pathway and cGMP-PKG

signaling. In particular, relaxin signaling pathway (Diaz et al., 2020; Ikeda et al., 2018) and cGMP-PKG signaling (d'Emmanuele di Villa Bianca et al., 2016) are linked to bladder contraction and the enrichment of these pathways at E16.5 and E18.5 coincides with the onset of urine production (Figure S9 A, Tables S4–S5).

Similarlyin the urethral epithelium, enriched pathways in the shared and early/mid categories showed a high degree of concordance. Enriched pathways included Wnt signaling, Notch signaling, Hippo signaling, Basal cell carcinoma and Pathways in cancer. Enriched pathways in the mid/late category included cancer and proliferation associated pathways including MAPK signaling pathway, prostate cancer and non-small cell lung cancer (Figure S9 B, Tables S6–S7).

3.5 The mesenchymal compartments of the developing bladder and urethra have spatially distinct gene expression patterns

To assess transcriptomic differences in bladder and urethra mesenchyme, we performed RNA-sequencing on isolated mesenchymal compartments from E16.5 embryos (Fig. 3 A). Principle component analysis showed samples segregated by tissue type and sex (Fig. 3 B). Assessment of differentially expressed genes in bladder and urethra mesenchyme revealed 4069 genes upregulated in bladder mesenchyme and 4274 genes upregulated in urethral mesenchyme (absolute log2 fold change of ≥0.5 and adjusted p-value of ≤0.01) (Fig. 3C,Table S10). We generated a heatmap of transcription factors that were differentially expressed in bladder and urethra mesenchymal compartments. *Pitx1, Pitx2, Gata5, Gata6, Elf4* and *Klf4* were differentially expressed in bladder mesenchyme while *Foxd2, Foxf2, Sox4, Sox11, Six1, Six4, Isl1* and *Hoxa13* were differentially expressed in urethral mesenchyme (Fig. 3 D). We further assessed the mesenchymal compartment at E14.5 and E18.5 by bulk-RNA sequencing (Figure S10 A-B, Figure S11 A-B, Tables S11–S12). The transcription factors *Pitx1, Pitx2, Gata6, Elf4* and *Klf4* show higher expression in the bladder mesenchyme at E14.5 and E18.5 suggesting that these are a core group of bladder mesenchyme specific transcription factors. In the urethral mesenchyme, *Foxd2, Foxf2, Sox4, Sox11, Six1, Six4, Isl1* and *Hoxa13* show higher expression at both E14.5 and E18.5 (Figure S10 C, Figure S11 C).

We performed immunostaining for the transcription factor KLF4 in the lower urinary tract. At E12.5, KLF4 is highly expressed in the epithelial lining of the bladder and urethra. Mesenchymal expression of KLF4 is higher in the developing bladder with a small patch on the ventral side of the urethra (Fig. 3 E). At E14.5 and E16.5, KLF4 expression has receded in the epithelium but is concentrated in the mesenchymal compartment of the bladder. At E14.5, KLF4 expression is widespread in the bladder mesenchyme (Fig. 3 F) but at E16.5 is confined to the lamina propria layer of the bladder (Fig. 3G–H). We tested the spatial distribution of *Pitx2* by *in situ* hybridization and found that expression was confined to the bladder mesenchyme and ventral side of the urethra at E12.5 (Fig. 3 I). At E16.5, expression is concentrated in the bladder smooth muscle layer with low expression in the urethral mesenchyme except for regions which correspond to the thin bands of smooth muscle in the urethra (Fig. 3J–K). To test whether these transcription factors are expressed earlier than E16.5, we performed expression analysis on select transcription factors at E14.5.

We confirmed the higher expression of *Pitx1, Pitx2, Gata6, Elf4* and *Klf4* in the bladder mesenchyme at E14.5 compared to the urethral mesenchyme by independent validation through qPCR and RNA-sequencing (Fig. 3 L, Figure S10 C).

To validate genes that were identified to be differentially expressed in the urethral mesenchyme, we performed qPCR for the transcription factor *Sox11* at E14.5 and identified that it had increased expression in the urethral mesenchyme compared to the bladder mesenchyme (Fig. 3 M). Further, *in situ* hybridization confirmed the expression of *Sox11* in urethral mesenchyme and not bladder mesenchyme at E12.5 and E16.5 (Fig. 3N–O). *Sox11* expression was also observed in the basal layer of the urethral epithelium (Figs. 3O–. 2 A). qPCR of transcription factors *Isl1, Foxd2* and *Foxf2* also revealed increased expression of these genes in urethral mesenchyme compared to bladder mesenchyme at E14.5 (Fig. 3P–R, Figure S10 C). We performed immunostaining for SIX1 (Fig. 3S–V) and PROM1 (Fig. 3W–Z), which were identified to be differentially expressed in urethral mesenchyme and found that protein expression was consistently higher in urethral mesenchyme compared to bladder mesenchyme at E12.5, E14.5 and E16.5.

3.6 Differential expression of developmental signaling pathway genes in urethra and bladder mesenchyme

We then examined the expression pattern of Wnt pathway genes in urethra and bladder mesenchyme. Wnt signaling has been implicated in several developmental processes including establishment of the anterior-posterior axis (Hikasa and Sokol, 2013) and formation of kidneys (Park et al., 2007) and lungs (Goss et al., 2009). We curated heatmaps of differentially expressed Wnt ligands, receptors and co-receptors in urethra and bladder mesenchyme. Wnt ligands *Wnt5a* and *Wnt11* showed increased expression in E16.5 urethra mesenchyme along with Wnt receptors *Fzd1, Fzd5, Fzd7, Fzd9* and *Fzd10. Wnt2* and *Wnt2b* showed increased expression in E16.5 bladder mesenchyme along with *Fzd4* and *Lgr6* (Fig. 4 A). *Wnt2, Wnt2b* and *Fzd4* also showed elevated expression in the bladder mesenchyme at both E14.5 and E18.5 (Figure S10 D, S11 D). We observed increased expression of several Wnt inhibitors *Dkk2, Wif1, Sfrp1, Sfrp2* and *Sfrp5* in urethral mesenchyme (Fig. 4 B). *Dkk2*, but not other Wnt inhibitors, was differentially expressed at E14.5 and E18.5 (Figure S10 D, S11 D). Wnt agonists *Rspo2* and *Rspo3* showed higher expression in urethral mesenchyme while *Rspo1* had increased expression in bladder mesenchyme (Fig. 4 C).

We assessed the pattern of *Wnt2* mRNA expression at E12.5, E14.5 and E16.5. *Wnt2* expression could be seen marking the developing bladder mesenchyme at E12.5 (Fig. 4 D). At E14.5 and E16.5, *Wnt2* was restricted to the lamina propria layer of the bladder and was excluded from bladder smooth muscle (Fig. 4E–G). We then performed *in situ* hybridization for *Wnt5a* at E12.5 and E15.5. *Wnt5a* has been previously implicated in genital tubercle development (Yamaguchi et al., 1999). *Wnt5a* expression was higher in the urethral mesenchyme at E14.5, E16.5 and E18.5 (Fig. 4 A, Figure S10 D, Figure S11 D). At E12.5, *Wnt5a* expression was observed in the genital tubercle mesenchyme and on the dorsal aspect of the urogenital sinus (Fig. 4 H). At E15.5, *Wnt5a* was strongly expressed on the dorsal urethral mesenchyme and to some extent on the ventral side of the urethra. *Wnt5a* expression was absent in bladder mesenchyme (Fig. 4 I). Using qPCR, we confirmed

increased expression of *Wnt2, Wnt2b* and *Lgr6* in bladder mesenchyme at E14.5. *Wnt5a, Fzd10, Dkk2, Rspo2* and *Rspo3* showed increased expression in E14.5 urethral mesenchyme (Fig. 4 J).

The Bmp/Smad pathway has been implicated in development of organs such as lung (Weaver et al., 1999), external genitalia (Suzuki et al., 2003; Xu et al., 2012) and prostate (Lamm et al., 2001). We observed increased expression of Bmp ligands *Bmp2, Bmp4* and *Bmp7* in urethral mesenchyme along with higher expression of *Smad1, Smad5, Smad7* and *Smad9*. Ligands *Bmp3, Bmp5, Bmp6* and *Bmp10* showed higher expression in bladder mesenchyme (Fig. 4 K). Using qPCR, we further confirmed increased expression of *Bmp2, Bmp4* and *Bmp7* in the urethral mesenchyme at E14.5 (Fig. 4 L).

Corresponding with increased expression of Notch receptors *Notch1, Notch2*, and *Notch3* (Figure S5 B) in urethral epithelium, transcriptomic analysis of the mesenchymal compartments revealed higher expression of Notch ligands *Jag1, Dll1, Dll3* and *Dll4* in urethral mesenchyme compared to bladder mesenchyme (Fig. 4 M). We identified differential expression of growth factors and receptors in urethra and bladder mesenchyme. Expression of ligands *Fgf10, Fgf13* and *Hgf* and the receptor *Fgfr1* were increased in urethral mesenchyme while *Igf2, Fgf5* and the receptor *Igf2r* were upregulated in bladder mesenchyme (Fig. 4 N).

3.7 The urethral epithelium shows higher expression of chemokines and barrier function genes compared to the bladder epithelium

We observed an enrichment of immune related pathways among genes showing higher expression in the E16.5 urethral epithelium. There was a strong enrichment of the TNF signaling pathway and a weaker enrichment for the pathways NF-kappa B signaling pathway, Chemokine signaling pathway and IL-17 signaling pathway (Fig. 1U,Table S7). Due to its proximity to the outside environment, we hypothesized that the urethral epithelial lining functions as an immune barrier. Barrier epithelia like the skin (Trompette and Ubags, 2023) and gut lining (Daneman and Rescigno, 2009) act as active innate immune barriers by creating physical and biochemical impediments to pathogens. Previous work has revealed the constitutive expression of immunomodulatory genes in the adult urethral lining (Henry et al., 2018; Joseph et al., 2020). We assessed the developmental expression of immune signaling and barrier function genes in the urethra and bladder epithelium from E16.5 embryos. Urethral epithelium displayed higher expression of the chemokine genes *Cx3cl1, Cxcl5, Cxcl14, Cxcl15, Cxcl16* and *Cxcl17* compared to the bladder epithelium (Fig. 5 A). We performed qPCR to validate expression of select chemokines *Cx3cl1* (Fig. 5 B), *Cxcl14* (Fig. 5 C), *Cxcl15* (Fig. 5 D) and *Cxcl16* (Fig. 5 E) in an independent set of E16.5 epithelial samples. Chemokine expression was consistently higher in the urethral epithelium compared to the bladder epithelium. *Cx3cl1* is a chemoattractant that binds to the chemokine receptor *Cx3cr1* expressed on myeloid lineage cells. We observed that the embryonic bladder epithelium is devoid of epithelial-associated embryonic macrophages at E16.5 (Fig. 5 F) and E18.5 (Fig. 5 H). In contrast, we observed several epithelial-associated macrophages in the urethra at E16.5 (Fig. 5 G) and E18.5 (Fig. 5 I). Epithelial associated macrophages increased in number in the adult urethral epithelium,

while the bladder epithelium remained devoid of macrophages (Fig. 5 J–K). The presence of urethral epithelial-associated macrophages correlates with increased expression of *Cx3cl1* and other chemokines in the urethral epithelium starting from embryonic stages. mRNA for *Cx3cl1* localized to the urethral epithelium at E14.5, E16.5 and adult stages with minimal expression in the bladder epithelium (Fig. 5L–T). The average amount of *Cx3cl1* mRNA gradually increased from embryonic to adult stages (Fig. 5N–Q, T) which correlated with increasing numbers of epithelial-associated macrophages in the urethra over the course of development. Additionally, the E16.5 urethral epithelium had higher expression of genes encoding tight junction proteins claudins *Cldn3, Cldn6, Cldn9* and gap junction proteins *Gja3* and *Gja8*. Mucins (*Muc1, Muc2, Muc4*, and *Muc20*) and genes involved in innate immunity (*Lcn2, Scgb1a1, Pglyrp3, Reg3g, Reg3b* and *Mmp7*) also showed higher expression in the urethral epithelium compared to the bladder epithelium (Figure S5 D). E18.5 urethral epithelium displayed higher expression of barrier function genes compared to bladder epithelium (Figure S8 E, Table S9). Differential expression of barrier function genes was absent at E14.5 (Table S8) suggesting that these genes are acquired during mid/late differentiation of the lower urinary tract. Our results indicate that developmental gene expression patterns position the urethral epithelium as an active immune barrier with closely associated immune cells.

3.8 The epithelial and mesenchymal compartments of the developing urethra show sexually dimorphic gene expression patterns

The urethra shows sex-specific differences during development (Georgas et al., 2015). The male urethra is elongated compared to the female urethra and this occurs in response to testosterone produced by the male gonads (Larkins et al., 2016). Hematoxylin and eosin staining on E18.5 and adult mouse lower urinary tracts was performed to highlight the morphological differences between the male and female urethra (Fig. S12). We tested whether sex-specific differences were present in male and female urethra and bladder epithelium. There were very few differentially expressed genes between male and female bladder epithelium (absolute log2 fold change of ≥0.5 and adjusted p-value of ≤0.01) (Fig. 6 A, Figure S13 A, Table S13). In contrast, there were 1096 upregulated genes in male urethral epithelium and 637 genes increased in female urethral epithelium (Fig. 6 B, Figure S13 B, Table S14). We curated a heatmap of select genes increased in male and female urethral epithelium. Some of these included prostate associated genes *Klk10, Ly6a, Psca* and *Nkx3-1* (Joseph et al., 2020) expressed in the male urethral epithelium. Additionally, barrier function genes Polymeric Immunoglobulin receptor *Pigr* (Lin et al., 2023) and the mucins *Muc4* and *Muc20* (Breugelmans et al., 2022) also showed increased expression in the male urethral epithelium. *Krt17*, Estrogen receptor 2 (*Esr2*) and the growth factors *Fgf3* and *Fgf9* showed increased expression in female urethral epithelium (Fig. 6 C). We performed independent validation of a subset of male and female urethral epithelial specific genes using qPCR (Fig. 6 D–E).

We then compared gene expression differences in male and female mesenchymal compartments of bladder and urethra. We observed minimal differentially expressed genes upon comparing male and female bladder mesenchyme (absolute log2 fold change of ≥0.5 and adjusted p-value of ≤0.01) (Fig. 6 F, Figure S13 C, Table S15). In contrast, there were

505 genes upregulated in male urethral mesenchyme and 268 genes upregulated in female urethral mesenchyme (Fig. 6 G, Figure S13 D, Table S16). *Aldh1a1*, which is associated with prostate development (Vezina et al., 2008), is increased in male urethral mesenchyme. Additionally, *Sfrp2, Srd5a2, Wif1, Rspo3, Rgs2, Apod* and *Sult1e1* are increased in male urethral mesenchyme. *Dkk2, Sall1* and *Rspo2* were some of the genes that showed increased expression in female urethral mesenchyme (Fig. 6 H). Independent validation of female and male urethral mesenchyme specific genes was done using qPCR (Fig. 6 I–J).

4 Discussion

In this study, we provide a direct comparison of gene expression in the urethra and bladder during development. We identified epithelial and mesenchymal genes that are specific to the developing bladder or urethra. Previous studies have addressed bladder development in isolation from the urethra. By providing a direct comparison of gene expression in the epithelial and mesenchymal compartments of the lower urinary tract, we have identified novel marker genes, transcription factors and signaling pathway genes that are spatially restricted to the bladder or urethra. Additionally, we identified a novel signature of chemokine gene expression in the urethral epithelium which correlated with the appearance of epithelial-associated macrophages. Lastly, our study revealed that the urethra shows sexually dimorphic gene expression in the epithelial and mesenchymal compartments while the bladder does not have the same degree of sexual dimorphism.

4.1 Early transcription factors expressed in the developing lower urinary tract

The bladder forms from the anterior aspect of the urogenital sinus (Georgas et al., 2015). We provide an immunohistochemical comparison of bladder and urethra differentiation from E12.5-E17.5 which shows tissue architecture and protein expression changes in the developing lower urinary tract (Fig. S1). Although the bladder and urethral epithelium are contiguous, there is a clear spatial distinction in epithelial differentiation. Early transcription factors that pattern the bladder are largely unknown. We observed a gradient of SOX2 expression in the lower urinary tract with the highest expression observed in the urethra. Bladder epithelium lacked SOX2 but expressed the transcription factor PPARG (Fig. S1). SOX2 and PPARG showed a mutually exclusive expression pattern in the lower urinary tract epithelium (Fig. S1). PPARG has been implicated in early bladder development and is known to induce FOXA1, IRF-1 (Varley et al., 2009) and GATA3 in the bladder epithelium (Warrick et al., 2016). However, FOXA1 and GATA3 are widespread in the developing urethra as well and may not represent bladder specific downstream effectors of PPARG. Additionally, we observed that GATA3 is widespread in the bladder epithelium prior to PPARG upregulation (Figure S1 B, Fig. 2 B). We identified that GATA2 expression forms a gradient with highest expression in the bladder epithelium and lower expression in the urethral epithelium. GATA2 is also expressed in intermediate mesoderm and GATA2 deficiency has previously been implicated in ureteric bud defects (Hoshino et al., 2008). GATA2 function has not been described in the urothelium. *Gata4, Foxs1, Foxj1, Irx4, Tbx2* and *Tbx22* also showed increased expression in bladder epithelium compared to urethral epithelium at E16.5 (Fig. 2 A). More differentially upregulated transcription factors were seen in the urethral epithelium with fewer in the bladder epithelium (Fig. 2 A). The handful

of transcription factor genes that are differentially expressed in bladder epithelium suggests a *de novo* epithelial differentiation program for bladder epithelium that is uncoupled from the urethral differentiation trajectory.

From our data, we identified *Irx1, Irx2* and *Pax9* as urethra specific transcription factors (Fig. 2). Irx genes have been implicated in regional patterning of tissues. *Irx1* and *Irx2* are co-expressed during limb development and downregulation of these genes by retinoic acid signaling correlates with the onset of cell death in inter-digital tissues (Díaz-Hernández et al., 2013). A previous study has also shown the concordance between gene networks involved in limb development and development of the external genitalia which contains the distal urethra (Chiu et al., 2010). In the lung, *Irx1* and *Irx2* play a role in proximal-distal morphogenesis as knockdown of these genes impaired branching (Tuyl et al., 2006). The restricted expression of *Irx1* and *Irx2* in the urethral epithelium prompts further investigation into the role of these transcription factors in lower urinary tract development. We identified *Pax9* as a novel transcription factor expressed in the urethral epithelium but absent from the bladder epithelium. *Pax9* is involved in tooth, limb and skeletal development where it is expressed in mesenchyme (Peters et al., 1998). In another barrier epithelial tissue, the esophagus, *Pax9* deficiency resulted in a loss of genes associated with squamous differentiation and an increase in cell proliferation and expression of the basal epithelial markers *Sox2* and *Tp63* (Xiong et al., 2018). *Pax9* may act to regulate epithelial differentiation in the urethral epithelium as well.

4.2 Defining gene signatures of the developing bladder and urethral epithelium

Our results provide a direct comparison between the bladder and urethral epithelium. The approach to use bulk-RNA sequencing enables us to understand broad gene expression signatures across epithelia. However, it lacks the cellular resolution of newer techniques like single cell RNA-sequencing. Currently, there are no published single cell RNA-sequencing datasets of the developing mouse urethra and bladder epithelium. We interrogated a published dataset (Qiu et al., 2024) that looked at gene expression signatures of single nuclei isolated from staged whole mouse embryos from gastrulation to birth. As whole embryos were pulverized for this study, the data does not retain any spatial identifiers of organ or tissue type. To test if we could identify bladder and urethral epithelium from this dataset, we created custom module scores from the gene signatures of bladder and urethral epithelium from our bulk RNA-sequencing data (Fig. S14, Table S2). Scoring was performed on E16.0-E16.75 cells in the published dataset which had been annotated by the authors as “Epithelial”. We were able to successfully identify distinct small groups of cells with high module scores for the bladder and urethral epithelium indicating the utility of the bulk RNA-sequencing dataset for annotating high resolution single cell datasets (Fig. S14).

4.3 Identification of bladder and urethra mesenchyme-specific genes

Previous studies have demonstrated the inductive capacity of embryonic bladder mesenchyme to induce bladder-specific epithelial differentiation (Joseph et al., 2018; Oottamasathien et al., 2007). Non-bladder cells in proximity to the bladder mesenchyme layer turn on bladder epithelial specific genes. This points to the existence of secreted signaling factors that selectively induce bladder- and not urethra-specific differentiation. We

identified *Wnt2* as an early expressed Wnt ligand in bladder mesenchyme (Fig. 4D–G). *Wnt2* expression selectively marks bladder mesenchyme as early as E12.5 and is gradually confined to fibroblasts in the lamina propria at later stages. *Wnt2* is often co-expressed with *Wnt2b* in other organs which we also observed in bladder mesenchyme (Fig. 4 J). In the lung, *Wnt2/2b* are involved in specification of *Nkx2.1* expressing lung progenitors from the endoderm and deletion of *Wnt2/2b* results in lung agenesis. Ablation of beta-catenin in the developing foregut also results in lung agenesis by promoting SOX2+ digestive progenitors over lung progenitors (Goss et al., 2009). *Wnt2* is essential for maintenance of zonation in the liver as depletion of this gene results in ablation of beta-catenin signaling and disruption of hepatocyte gene expression (Hu et al., 2022). Disruption of Wnt signaling in the endoderm results in a defect in cloacal septation and arrested development of the bladder (Mehta et al., 2013). Based on this evidence, *Wnt2/2b* may promote increased Wnt signaling in the developing bladder and also suppress SOX2+ urethral identity. *Wnt2* can act as a ligand for receptor *Fzd4* (Yin et al., 2021). From our data, *Fzd4* is highly expressed in bladder mesenchyme compared to urethral mesenchyme (Fig. 4 A). *Wnt2* may act autonomously to direct differentiation of bladder mesenchyme. Alternatively, *Fzd5* is expressed in the bladder epithelium and may serve as the receptor for *Wnt2* (Figure S5 C).

Expression of the transcription factor gene *Klf4* followed a similar spatial pattern to *Wnt2* and was localized exclusively to bladder mesenchyme. At later stages of development, KLF4 protein expression became confined to the lamina propria layer of the bladder mesenchyme. There is evidence that the embryonic bladder is hypoxic (Burgu et al., 2007) and *Klf4* has been shown to be regulated by hypoxia (Shan et al., 2020). In the lung, *Klf4* expression regulates differentiation of myofibroblasts and fibroblasts by inducing expression of smooth muscle actin, tenascin C and genes encoding extracellular matrix proteins (Jean et al., 2013). Further investigation is required to attribute functions to KLF4 in bladder development.

Our transcriptomic data showed increased expression of the transcription factors *Gata5, Gata6, Pitx1* and *Pitx2* in bladder mesenchyme. *In vitro* studies have implicated *Gata6* in bladder smooth muscle development (Kanematsu et al., 2007). *Gata5* has been described in the genitourinary system but has not been studied in the context of bladder development. Female mice lacking *Gata5* show vaginal, uterine and urethral defects (Molkentin et al., 2000). In the cardiovascular system, *Gata5* is required for specification of myocardial precursors (Reiter et al., 1999). *Gata5* may perform a similar function in the bladder by regulating muscle development. *Pitx2* has been known to regulate muscle development but has not been studied in the bladder (L'Honoré et al., 2007). *Pitx2* could be a novel gene involved in bladder smooth muscle differentiation.

Differential expression of genes involved in the Wnt, Bmp, Notch and growth factor signaling pathways were observed in the bladder and urethral mesenchyme. Genes for several Wnt pathway inhibitors including *Dkk2, Wif1, Sfrp1, Sfrp2* and *Sfrp5* were increased in the urethral mesenchyme (Fig. 4 B). Interestingly, urethra or bladder specific expression of Wnt ligands and receptors was observed in both the epithelial and mesenchymal compartments (Fig. 4A,S5 C). Wnt and R-spondin gene expression patterns in the developing urethra and prostate have been extensively characterized by Mehta et al. (2011). Our work complements this study by extending to Wnt pathway genes in

the bladder. Notch pathway ligands *Dll1, Dll3* and *Dll4* showed increased expression in the urethral mesenchyme compared to the bladder mesenchyme (Fig. 4 M) and this corresponded with increased expression of the receptors *Notch1, Notch2* and *Notch3* in the urethral epithelium (Figure S5 B).

4.4 Developmental signatures in cancer

Developmental programs are reactivated during tumor development (Xue et al., 2020). PPARG, an early marker of bladder differentiation has been implicated in bladder cancer (Rochel et al., 2019). In mice, expression of an active form of Pparg in basal cells is sufficient to turn basal tumors to a luminal subtype (Tate et al., 2021). Luminal tumors also express KRT20 and Uroplakin (Guo et al., 2020) that are developmentally expressed. PPARG interestingly suppressed the NF-kB program in these cells making it immunologically cold (Tate et al., 2021). Another study (Lai et al., 2021) described a patient with muscle invasive bladder cancer who had an epithelial sub-population marked by KRT13, SOX2 and SOX9. In the dataset in the current manuscript, this is a signature for urethral cells (Table S2) and potentially marks a deviation from transitional urothelium to stratified epithelium of the urethral type in certain sub-types of bladder cancer.

Our analysis of KEGG pathways in the developing urethral epithelium shows enrichment of several cancer related pathways and a pluripotency related pathway. Wnt signaling pathway, which has been implicated in cancer (Sanchez-Vega et al., 2018), was highly enriched in the urethral epithelium (Fig. 1 U, Figure S9 B, Table S7). This highlights the less differentiated and more primitive state of the urethral epithelium compared to the bladder epithelium at this stage.

4.5 Gene expression in the urethral epithelium points to its role as a mechanical and immune barrier

The function of the mature urethral epithelium is to act as a conduit and its proximity to the outside environment necessitates a distinct set of features to contend with environmental insults. Higher expression of a variety of keratins *Krt4, Krt13, Krt14* and *Krt17* (Fig. 1 D) in the urethral epithelium points to increased keratinization compared to the bladder. We found that the urethral epithelium expresses the anti-apoptotic gene *Bcl2* (Fig. 1E–H) which may aid in surviving dissociation mediated apoptosis from urine shear stress. *Bcl2* is also expressed in the basal layer of other stratified epithelium like the skin (Rodriguez-Villanueva et al., 1995) and esophagus (Sarbia et al., 1996). The urethral lining also expresses the enzyme Arginase-1 (Arg*1*). *Arg1* is widely studied in the context of alternatively activated macrophages and has been shown to play a role in the wound healing response in skin (Campbell et al., 2013; Crompton et al., 2022). *Arg1* can regulate production of polyamines by catalyzing the conversion of L-arginine to ornithine which is require for polyamine generation (Kropf et al., 2005). *Arg1* expression during urethral development could indicate a role in organogenesis.

In addition to its function as a conduit, the urethra has emerging functions as an immune barrier. Previous work has shown that human urethral epithelial cells have a distinct antimicrobial and innate immune gene expression signature that may act as a deterrent

for urinary pathogens (Joseph et al., 2020). In this study, we observed higher expression of the chemokine genes *Cx3cl1, Cxcl5, Cxcl14, Cxcl15, Cxcl16* and *Cxcl17* in the mouse urethral epithelium compared to the bladder epithelium (Fig. 5 A). The expression of immunomodulatory genes appears to be intrinsic to the urethral epithelial differentiation program as the embryos have not yet encountered the external environment or been exposed to inflammatory stimuli. Similar to the urethral epithelium, *Cx3cl1* is expressed by the intestinal epithelium (Muehlhoefer et al., 2000). Loss of epithelial CX3CL1 prevents CX3CR1+ immune cells from sending transepithelial dendrites across the intestinal barrier to sample the external environment (Kim et al., 2011). We see a similar localization of *Cx3cl1* expression to the urethral epithelium at embryonic and adult stages. This correlates with homing of increasing numbers of epithelial-associated macrophages with dendritic morphology to the urethral epithelium (Fig. 5).

During late fetal stages and in increasing numbers in the adult, macrophages enter the urethral lining and extend dendritic projections between epithelial membranes (Fig. 5 K). Langerhans cells in the skin exhibit transepithelial dendrite extension and retraction during homeostasis (Nishibu et al., 2006) and have been shown to penetrate epithelial tight junctions for antigen sampling (Yoshida et al., 2014). It is unclear what allows association of epithelial-associated immune cells with epithelial cells. Although Langerhans cells express E-cadherin (Blauvelt et al., 1995), it has been shown to be dispensable for their association with epithelium (Brand et al., 2020). Gut dendritic cells express tight junction proteins that enable them to penetrate the gut epithelium to sample bacteria (Rescigno et al., 2001). Expression of junction proteins by immune cells may be required to maintain contact with epithelial cells and prevent disruption of the barrier.

Macrophage interactions with multiple cell types have been shown to be important for tissue homeostasis and remodeling. Macrophage interaction with myocytes through gap junctions promotes electric conductance in the heart (Hulsmans et al., 2017). Macrophages aid in anastomosis of newly formed blood vessels by interaction with endothelial cells (Fantin et al., 2010). The association of macrophages with urethral epithelial cells could promote barrier function. In the gut, epithelial-associated macrophages sample fungal antigens from the lumen to reduce stress on epithelial cells and depletion of macrophages compromises epithelial barrier integrity (Chikina et al., 2020). Urethral epithelial macrophages could potentially perform a similar role in the lower urinary tract by sampling antigens from the lumen for detection of pathogens.

The establishment of the immune niche in the urethra was previously unexplored. In this study, we provide evidence for the role of fetal urethral epithelium in regulating the immune niche. Future studies are required to test the direct role of *Cx3cl1* in homing and invasion of immune cells into the urethral epithelium during development and the maintenance of this niche under homeostasis. Additionally, the urethral epithelium expresses several antimicrobial peptides like *Reg3b, Reg3g* (Udomsopagit et al., 2020) and genes involved in innate immunity like *Mmp7* (Vandenbroucke et al., 2014), *Pglyrp3* (Zenhom et al., 2011) and *Lcn2* (Flo et al., 2004). This points to the specialization of the urethral epithelium during development and its role as an underexplored immune barrier.

Overall, our study provides keys insights into lower urinary tract development by providing a direct comparison of gene expression in the epithelial and mesenchymal compartments of the developing bladder and urethra. This direct comparison of the bladder to the urethra allows us to identify candidate genes that may direct bladder- or urethraspecific differentiation for future applications in regenerative therapies.

Supplementary Material

Refer to Web version on PubMed Central for supplementary material.

Acknowledgements

The authors would like to thank Dr. Douglas Strand (UT Southwestern Medical Center), Dr. Chad Vezina (University of Wisconsin-Madison) and Dr. Apurva Sarin for sharing antibodies and primers. We would like to thank Dr. Douglas Strand and Dr. Soman Abraham (Duke University) for their helpful suggestions on the manuscript. We acknowledge the Next Generation Genomics Facility (NGGF) and the Animal Care and Resource Centre at the Bangalore Life Science Cluster (BLiSC) for their services.

Funding

This work was supported by DBT/Wellcome Trust India Alliance Early Career Fellowship (Ref: IA/E/21/1/506274) to D.B.J. and Department of Biotechnology (DBT), Government of India Institutional core funds to inStem.

Data availability

Data will be made available on request.

References

Abler LL, Mehta V, Keil KP, Joshi PS, Flucus CL, Hardin HA, Schmitz CT, Vezina CM. A high throughput in situ hybridization method to characterize mRNA expression patterns in the fetal mouse lower urogenital tract. J Vis Exp. 2011; 54: 2912. doi: 10.3791/2912 [PubMed: 21876526]

Amato CM, Yao HH-C. Developmental and sexual dimorphic atlas of the prenatal mouse external genitalia at the single-cell level. Proc Natl Acad Sci USA. 2021; 118 e2103856118 doi: 10.1073/pnas.2103856118 [PubMed: 34155146]

Bae S-K, Bessho Y, Hojo M, Kageyama R. The bHLH gene Hes6, an inhibitor of Hes1, promotes neuronal differentiation. Development. 2000; 127: 2933–2943. [PubMed: 10851137]

Baskin L, DiSandro M, Li Y, Li W, Hayward S, Cunha G. Mesenchymal-epithelial interactions in bladder smooth muscle development: effects of the local tissue environment. J Urol. 2001; 165: 1283–1288. [PubMed: 11257702]

Blauvelt A, Katz SI, Udey MC. Human langerhans cells express E-cadherin. J Invest Dermatol. 1995; 104: 293–296. [PubMed: 7829887]

Brand A, Diener N, Zahner SP, Tripp C, Backer RA, Karram K, Jiang A, Mellman I, Stoitzner P, Clausen BE. E-cadherin is dispensable to maintain langerhans cells in the epidermis. J Invest Dermatol. 2020; 140: 132–142. e133 [PubMed: 31260672]

Breugelmans T, Oosterlinck B, Arras W, Ceuleers H, De Man J, Hold GL, De Winter BY, Smet A. The role of mucins in gastrointestinal barrier function during health and disease. The Lancet Gastroenterology & Hepatology. 2022; 7: 455–471. [PubMed: 35397245]

Burgu B, Medina Ortiz WE, Pitera JE, Woolf AS, Wilcox DT. Vascular endothelial growth factor mediates hypoxic stimulated embryonic bladder growth in organ culture. J Urol. 2007; 177: 1552–1557. [PubMed: 17382777]

Campbell L, Saville CR, Murray PJ, Cruickshank SM, Hardman MJ. Local Arginase 1 activity is required for cutaneous wound healing. J Invest Dermatol. 2013; 133: 2461–2470. DOI: 10.1038/jid.2013.164 [PubMed: 23552798]

Cao M, Liu B, Cunha G, Baskin L. Urothelium patterns bladder smooth muscle location. Pediatr Res. 2008; 64: 352–357. DOI: 10.1203/PDR.0b013e318180e4c9 [PubMed: 18535485]

Cao M, Tasian G, Wang MH, Liu B, Cunha G, Baskin L. Urothelium-derived Sonic hedgehog promotes mesenchymal proliferation and induces bladder smooth muscle differentiation. Differentiation. 2010; 79: 244–250. DOI: 10.1016/j.diff.2010.02.002 [PubMed: 20227816]

Carmichael SL, Ma C, Choudhry S, Lammer EJ, Witte JS, Shaw GM. Hypospadias and genes related to genital tubercle and early urethral development. J Urol. 2013; 190: 1884–1892. DOI: 10.1016/j.juro.2013.05.061 [PubMed: 23727413]

Cheng W, Yeung CK, Ng YK, Zhang JR, Hui CC, Kim PC. Sonic Hedgehog mediator Gli2 regulates bladder mesenchymal patterning. J Urol. 2008; 180: 1543–1550. [PubMed: 18710724]

Chikina AS, Nadalin F, Maurin M, San-Roman M, Thomas-Bonafos T, Li XV, Lameiras S, Baulande S, Henri S, Malissen B, Lacerda Mariano L, et al. Macrophages maintain epithelium integrity by limiting fungal product absorption. Cell. 2020; 183: 411–428. e416 doi: 10.1016/j.cell.2020.08.048 [PubMed: 32970988]

Chiu HS, Szucsik JC, Georgas KM, Jones JL, Rumballe BA, Tang D, Grimmond SM, Lewis AG, Aronow BJ, Lessard JL, Little MH. Comparative gene expression analysis of genital tubercle development reveals a putative appendicular Wnt7 network for the epidermal differentiation. Dev Biol. 2010; 344: 1071–1087. DOI: 10.1016/j.ydbio.2010.05.495 [PubMed: 20510229]

Crompton RA, Williams H, Campbell L, Hui Kheng L, Saville C, Ansell DM, Reid A, Wong J, Vardy LA, Hardman MJ, Cruickshank SM. An epidermal-specific role for Arginase1 during cutaneous wound repair. J Invest Dermatol. 2022; 142: 1206–1216. e1208 [PubMed: 34710388]

Cunha GR, Vezina CM, Isaacson D, Ricke WA, Timms BG, Cao M, Franco O, Baskin LS. Development of the human prostate. Differentiation. 2018; 103: 24–45. DOI: 10.1016/j.diff.2018.08.005 [PubMed: 30224091]

d'Emmanuele di Villa Bianca R, Mitidieri E, Fusco F, Russo A, Pagliara V, Tramontano T, Donnarumma E, Mirone V, Cirino G, Russo G, Sorrentino R. Urothelium muscarinic activation phosphorylates CBSSer227 via cGMP/PKG pathway causing human bladder relaxation through H2S production. Sci Rep. 2016; 6 31491 doi: 10.1038/srep31491 [PubMed: 27509878]

Daneman R, Rescigno M. The gut immune barrier and the blood-brain barrier: are they so different? Immunity. 2009; 31: 722–735. [PubMed: 19836264]

Danopoulos S, Alonso I, Thornton ME, Grubbs BH, Bellusci S, Warburton D, Al Alam D. Human lung branching morphogenesis is orchestrated by the spatiotemporal distribution of ACTA2, SOX2, and SOX9. Am J Physiol Lung Cell Mol Physiol. 2018; 314: L144–l149. DOI: 10.1152/ajplung.00379.2017 [PubMed: 28971977]

Díaz-Hernández ME, Bustamante M, Galván-Hernández CI, Chimal-Monroy J. Irx1 and Irx2 are coordinately expressed and regulated by retinoic acid, TGFβ and FGF signaling during chick hindlimb development. PLoS One. 2013; 8 e58549 doi: 10.1371/journal.pone.0058549 [PubMed: 23505533]

Diaz EC, Briggs M, Wen Y, Zhuang G, Wallace SL, Dobberfuhl AD, Kao C-S, Chen BC. Characterizing relaxin receptor expression and exploring relaxin's effect on tissue remodeling/fibrosis in the human bladder. BMC Urol. 2020; 20: 44. doi: 10.1186/s12894-020-00607-4 [PubMed: 32321501]

Elias PM. The skin barrier as an innate immune element. Semin Immunopathol. 2007; 29: 3–14. [PubMed: 17621950]

Fantin A, Vieira JM, Gestri G, Denti L, Schwarz Q, Prykhozhij S, Peri F, Wilson SW, Ruhrberg C. Tissue macrophages act as cellular chaperones for vascular anastomosis downstream of VEGF-mediated endothelial tip cell induction. Blood. 2010; 116: 829–840. DOI: 10.1182/blood-2009-12-257832 [PubMed: 20404134]

Flo TH, Smith KD, Sato S, Rodriguez DJ, Holmes MA, Strong RK, Akira S, Aderem A. Lipocalin 2 mediates an innate immune response to bacterial infection by sequestrating iron. Nature. 2004; 432: 917–921. [PubMed: 15531878]

Gandhi D, Molotkov A, Batourina E, Schneider K, Dan H, Reiley M, Laufer E, Metzger D, Liang F, Liao Y, Sun TT, et al. Retinoid signaling in progenitors controls specification and regeneration

Europe PMC Funders Author Manuscripts

of the urothelium. Dev Cell. 2013; 26: 469–482. DOI: 10.1016/j.devcel.2013.07.017 [PubMed: 23993789]

Ge SX, Jung D, Yao R. ShinyGO: a graphical gene-set enrichment tool for animals and plants. Bioinformatics. 2020; 36: 2628–2629. DOI: 10.1093/bioinformatics/btz931 [PubMed: 31882993]

Georgas KM, Armstrong J, Keast JR, Larkins CE, McHugh KM, Southard-Smith EM, Cohn MJ, Batourina E, Dan H, Schneider K, Buehler DP, et al. An illustrated anatomical ontology of the developing mouse lower urogenital tract. Development. 2015; 142: 1893–1908. DOI: 10.1242/dev.117903 [PubMed: 25968320]

Goss AM, Tian Y, Tsukiyama T, Cohen ED, Zhou D, Lu MM, Yamaguchi TP, Morrisey EE. Wnt2/2b and beta-catenin signaling are necessary and sufficient to specify lung progenitors in the foregut. Dev Cell. 2009; 17: 290–298. DOI: 10.1016/j.devcel.2009.06.005 [PubMed: 19686689]

Guha A, Vasconcelos M, Cai Y, Yoneda M, Hinds A, Qian J, Li G, Dickel L, Johnson JE, Kimura S, Guo J, et al. Neuroepithelial body microenvironment is a niche for a distinct subset of Clara-like precursors in the developing airways. Proc Natl Acad Sci USA. 2012; 109: 12592–12597. DOI: 10.1073/pnas.1204710109 [PubMed: 22797898]

Guo CC, Bondaruk J, Yao H, Wang Z, Zhang L, Lee S, Lee J-G, Cogdell D, Zhang M, Yang G, Dadhania V, et al. Assessment of luminal and basal phenotypes in bladder cancer. Sci Rep. 2020; 10 9743 doi: 10.1038/s41598-020-66747-7 [PubMed: 32546765]

Hadley, W. ggplot2: Elegant Graphics for Data Analysis. Springer-Verlag; New York: 2016.

Henry GH, Malewska A, Joseph DB, Malladi VS, Lee J, Torrealba J, Mauck RJ, Gahan JC, Raj GV, Roehrborn CG, Hon GC, et al. A cellular anatomy of the normal adult human prostate and prostatic urethra. Cell Rep. 2018; 25: 3530–3542. e3535 doi: 10.1016/j.celrep.2018.11.086 [PubMed: 30566875]

Hikasa H, Sokol SY. Wnt signaling in vertebrate axis specification. Cold Spring Harbor Perspect Biol. 2013; 5 a007955 doi: 10.1101/cshperspect.a007955 [PubMed: 22914799]

Hoshino T, Shimizu R, Ohmori S, Nagano M, Pan X, Ohneda O, Khandekar M, Yamamoto M, Lim K-C, Engel JD. Reduced BMP4 abundance in Gata2 hypomorphic mutant mice result in uropathies resembling human CAKUT. Gene Cell. 2008; 13: 159–170. [PubMed: 18233958]

Hu S, Liu S, Bian Y, Poddar M, Singh S, Cao C, McGaughey J, Bell A, Blazer LL, Adams JJ, Sidhu SS, et al. Single-cell spatial transcriptomics reveals a dynamic control of metabolic zonation and liver regeneration by endothelial cell Wnt2 and Wnt9b. Cell reports Medicine. 2022; 3 100754 doi: 10.1016/j.xcrm.2022.100754 [PubMed: 36220068]

Hulsmans M, Clauss S, Xiao L, Aguirre AD, King KR, Hanley A, Hucker WJ, Wülfers EM, Seemann G, Courties G, Iwamoto Y, et al. Macrophages facilitate electrical conduction in the heart. Cell. 2017; 169: 510–522. e520 doi: 10.1016/j.cell.2017.03.050 [PubMed: 28431249]

Ikeda Y, Zabbarova IV, Birder LA, Wipf P, Getchell SE, Tyagi P, Fry CH, Drake MJ, Kanai AJ. Relaxin-2 therapy reverses radiation-induced fibrosis and restores bladder function in mice. Neurourol Urodyn. 2018; 37: 2441–2451. DOI: 10.1002/nau.23721 [PubMed: 29806709]

Jean JC, George E, Kaestner KH, Brown LA, Spira A, Joyce-Brady M. Transcription factor Klf4, induced in the lung by oxygen at birth, regulates perinatal fibroblast and myofibroblast differentiation. PLoS One. 2013; 8 e54806 doi: 10.1371/journal.pone.0054806 [PubMed: 23372771]

Joseph DB, Chandrashekar AS, Abler LL, Chu LF, Thomson JA, Mendelsohn C, Vezina CM. In vivo replacement of damaged bladder urothelium by Wolffian duct epithelial cells. Proc Natl Acad Sci USA. 2018; 115: 8394–8399. DOI: 10.1073/pnas.1802966115 [PubMed: 30061411]

Joseph DB, Henry GH, Malewska A, Iqbal NS, Ruetten HM, Turco AE, Abler LL, Sandhu SK, Cadena MT, Malladi VS, Reese JC, et al. Urethral luminal epithelia are castration-insensitive cells of the proximal prostate. Prostate. 2020; 80: 872–884. DOI: 10.1002/pros.24020 [PubMed: 32497356]

Kanematsu A, Ramachandran A, Adam RM. GATA-6 mediates human bladder smooth muscle differentiation: involvement of a novel enhancer element in regulating alpha-smooth muscle actin gene expression. Am J Physiol Cell Physiol. 2007; 293: C1093–C1102. [PubMed: 17626241]

Karni-Schmidt O, Castillo-Martin M, Shen TH, Gladoun N, Domingo-Domenech J, Sanchez-Carbayo M, Li Y, Lowe S, Prives C, Cordon-Cardo C. Distinct expression profiles of p63 variants during

urothelial development and bladder cancer progression. Am J Pathol. 2011; 178: 1350–1360. DOI: 10.1016/j.ajpath.2010.11.061 [PubMed: 21356385]

Kim D, Paggi JM, Park C, Bennett C, Salzberg SL. Graph-based genome alignment and genotyping with HISAT2 and HISAT-genotype. Nat Biotechnol. 2019; 37: 907–915. DOI: 10.1038/s41587-019-0201-4 [PubMed: 31375807]

Kim K-W, Vallon-Eberhard A, Zigmond E, Farache J, Shezen E, Shakhar G, Ludwig A, Lira SA, Jung S. In vivo structure/function and expression analysis of the CX3C chemokine fractalkine. Blood. 2011; 118: e156–e167. DOI: 10.1182/blood-2011-04-348946 [PubMed: 21951685]

Kropf P, Fuentes JM, Fähnrich E, Arpa L, Herath S, Weber V, Soler G, Celada A, Modolell M, Müller I. Arginase and polyamine synthesis are key factors in the regulation of experimental leishmaniasis in vivo. Faseb J. 2005; 19: 1000–1002. [PubMed: 15811879]

L'Honoré A, Coulon V, Marcil A, Lebel M, Lafrance-Vanasse J, Gage P, Camper S, Drouin J. Sequential expression and redundancy of Pitx2 and Pitx3 genes during muscle development. Dev Biol. 2007; 307: 421–433. [PubMed: 17540357]

Lai H, Cheng X, Liu Q, Luo W, Liu M, Zhang M, Miao J, Ji Z, Lin GN, Song W, Zhang L, et al. Single-cell RNA sequencing reveals the epithelial cell heterogeneity and invasive subpopulation in human bladder cancer. Int J Cancer. 2021; 149: 2099–2115. [PubMed: 34480339]

Lamm ML, Podlasek CA, Barnett DH, Lee J, Clemens JQ, Hebner CM, Bushman W. Mesenchymal factor bone morphogenetic protein 4 restricts ductal budding and branching morphogenesis in the developing prostate. Dev Biol. 2001; 232: 301–314. [PubMed: 11401393]

Larkins CE, Enriquez AB, Cohn MJ. Spatiotemporal dynamics of androgen signaling underlie sexual differentiation and congenital malformations of the urethra and vagina. Proc Natl Acad Sci USA. 2016; 113: E7510–e7517. DOI: 10.1073/pnas.1610471113 [PubMed: 27821748]

Li H, Handsaker B, Wysoker A, Fennell T, Ruan J, Homer N, Marth G, Abecasis G, Durbin R. The sequence alignment/map format and SAMtools. Bioinformatics. 2009; 25: 2078–2079. DOI: 10.1093/bioinformatics/btp352 [PubMed: 19505943]

Liao Y, Smyth GK, Shi W. The Subread aligner: fast, accurate and scalable read mapping by seed-and-vote. Nucleic Acids Res. 2013; 41: e108. doi: 10.1093/nar/gkt214 [PubMed: 23558742]

Lin H, Lin J, Pan T, Li T, Jiang H, Fang Y, Wang Y, Wu F, Huang J, Zhang H, Chen D, et al. Polymeric immunoglobulin receptor deficiency exacerbates autoimmune hepatitis by inducing intestinal dysbiosis and barrier dysfunction. Cell Death Dis. 2023; 14: 68. doi: 10.1038/s41419-023-05589-3 [PubMed: 36709322]

Liu C, Tate T, Batourina E, Truschel ST, Potter S, Adam M, Xiang T, Picard M, Reiley M, Schneider K, Tamargo M, et al. Pparg promotes differentiation and regulates mitochondrial gene expression in bladder epithelial cells. Nat Commun. 2019; 10: 4589. doi: 10.1038/s41467-019-12332-0 [PubMed: 31597917]

Liu FT, Hsu DK, Zuberi RI, Kuwabara I, Chi EY, Henderson WR Jr. Expression and function of galectin-3, a beta-galactoside-binding lectin, in human monocytes and macrophages. Am J Pathol. 1995; 147: 1016–1028. [PubMed: 7573347]

Love MI, Huber W, Anders S. Moderated estimation of fold change and dispersion for RNA-seq data with DESeq2. Genome Biol. 2014; 15: 550. doi: 10.1186/s13059-014-0550-8 [PubMed: 25516281]

Matsumaru D, Murashima A, Fukushima J, Senda S, Matsushita S, Nakagata N, Miyajima M, Yamada G. Systematic stereoscopic analyses for cloacal development: the origin of anorectal malformations. Sci Rep. 2015; 5 13943 doi: 10.1038/srep13943 [PubMed: 26354024]

McAuley E, Moline D, VanOpstall C, Lamperis S, Brown R, Vander Griend DJ. Sox2 expression marks castration-resistant progenitor cells in the adult murine prostate. Stem Cell. 2019; 37: 690–700. DOI: 10.1002/stem.2987 [PubMed: 30720908]

Mehta V, Abler LL, Keil KP, Schmitz CT, Joshi PS, Vezina CM. Atlas of Wnt and R-spondin gene expression in the developing male mouse lower urogenital tract. Dev Dynam. 2011; 240: 2548–2560. DOI: 10.1002/dvdy.22741 [PubMed: 21936019]

Mehta V, Schmitz CT, Keil KP, Joshi PS, Abler LL, Lin TM, Taketo MM, Sun X, Vezina CM. Beta-catenin (CTNNB1) induces Bmp expression in urogenital sinus epithelium and

participates in prostatic bud initiation and patterning. Dev Biol. 2013; 376: 125–135. DOI: 10.1016/j.ydbio.2013.01.034 [PubMed: 23396188]

Molkentin JD, Tymitz KM, Richardson JA, Olson EN. Abnormalities of the genitourinary tract in female mice lacking GATA5. Mol Cell Biol. 2000; 20: 5256–5260. DOI: 10.1128/mcb.20.14.5256-5260.2000 [PubMed: 10866681]

Morgan EA, Nguyen SB, Scott V, Stadler HS. Loss of Bmp7 and Fgf8 signaling in Hoxa13-mutant mice causes hypospadia. Development. 2003; 130: 3095–3109. [PubMed: 12783783]

Muehlhoefer A, Saubermann LJ, Gu X, Luedtke-Heckenkamp K, Xavier R, Blumberg RS, Podolsky DK, MacDermott RP, Reinecker HC. Fractalkine is an epithelial and endothelial cell-derived chemoattractant for intraepithelial lymphocytes in the small intestinal mucosa. J Immunol. 2000; 164: 3368–3376. [PubMed: 10706732]

Nishibu A, Ward BR, Jester JV, Ploegh HL, Boes M, Takashima A. Behavioral responses of epidermal langerhans cells in situ to local pathological stimuli. J Invest Dermatol. 2006; 126: 787–796. [PubMed: 16439974]

Oliveros JC. Venny. An Interactive Tool for Comparing Lists with Venn's Diagrams. 2007; 2015

Oottamasathien S, Wang Y, Williams K, Franco OE, Wills ML, Thomas JC, Saba K, Sharif-Afshar A-R, Makari JH, Bhowmick NA, DeMarco RT, et al. Directed differentiation of embryonic stem cells into bladder tissue. Dev Biol. 2007; 304: 556–566. DOI: 10.1016/j.ydbio.2007.01.010 [PubMed: 17289017]

Opferman JT, Kothari A. Anti-apoptotic BCL-2 family members in development. Cell Death Differ. 2018; 25: 37–45. DOI: 10.1038/cdd.2017.170 [PubMed: 29099482]

Park JS, Valerius MT, McMahon AP. Wnt/beta-catenin signaling regulates nephron induction during mouse kidney development. Development. 2007; 134: 2533–2539. [PubMed: 17537789]

Perriton CL, Powles N, Chiang C, Maconochie MK, Cohn MJ. Sonic hedgehog signaling from the urethral epithelium controls external genital development. Dev Biol. 2002; 247: 26–46. [PubMed: 12074550]

Peters H, Neubüser A, Kratochwil K, Balling R. Pax9-deficient mice lack pharyngeal pouch derivatives and teeth and exhibit craniofacial and limb abnormalities. Genes Dev. 1998; 12: 2735–2747. DOI: 10.1101/gad.12.17.2735 [PubMed: 9732271]

Qiu C, Martin BK, Welsh IC, Daza RM, Le T-M, Huang X, Nichols EK, Taylor ML, Fulton O, O'Day DR, Gomes AR, et al. A single-cell time-lapse of mouse prenatal development from gastrula to birth. Nature. 2024; 626: 1084–1093. DOI: 10.1038/s41586-024-07069-w [PubMed: 38355799]

Reiter JF, Alexander J, Rodaway A, Yelon D, Patient R, Holder N, Stainier DY. Gata5 is required for the development of the heart and endoderm in zebrafish. Genes Dev. 1999; 13: 2983–2995. DOI: 10.1101/gad.13.22.2983 [PubMed: 10580005]

Rescigno M, Urbano M, Valzasina B, Francolini M, Rotta G, Bonasio R, Granucci F, Kraehenbuhl J-P, Ricciardi-Castagnoli P. Dendritic cells express tight junction proteins and penetrate gut epithelial monolayers to sample bacteria. Nat Immunol. 2001; 2: 361–367. [PubMed: 11276208]

Rochel N, Krucker C, Coutos-Thévenot L, Osz J, Zhang R, Guyon E, Zita W, Vanthong S, Hernandez OA, Bourguet M, Badawy KA, et al. Recurrent activating mutations of PPARγ associated with luminal bladder tumors. Nat Commun. 2019; 10: 253. doi: 10.1038/s41467-018-08157-y [PubMed: 30651555]

Rodriguez-Villanueva J, Colome MI, Brisbay S, McDonnell TJ. The expression and localization of bcl-2 protein in normal skin and in non-melanoma skin cancers. Pathol Res Pract. 1995; 191: 391–398. [PubMed: 7479356]

Sanchez-Vega F, Mina M, Armenia J, Chatila WK, Luna A, La KC, Dimitriadoy S, Liu DL, Kantheti HS, Saghafinia S, Chakravarty D, et al. Oncogenic signaling pathways in the cancer genome atlas. Cell. 2018; 173: 321–337. e310 doi: 10.1016/j.cell.2018.03.035 [PubMed: 29625050]

Sarbia M, Bittinger F, Porschen R, Verreet P, Dutkowski P, Willers R, Gabbert HE. bcl-2 expression and prognosis in squamous-cell carcinomas of the esophagus. Int J Cancer. 1996; 69: 324–328. [PubMed: 8797876]

Satija R, Farrell JA, Gennert D, Schier AF, Regev A. Spatial reconstruction of single-cell gene expression data. Nat Biotechnol. 2015; 33: 495–502. DOI: 10.1038/nbt.3192 [PubMed: 25867923]

Schneider AJ, Gawdzik J, Vezina CM, Baker TR, Peterson RE. Sox9 in mouse urogenital sinus epithelium mediates elongation of prostatic buds and expression of genes involved in epithelial cell migration. Gene Expr Patterns. 2019; 34 119075 doi: 10.1016/j.gep.2019.119075 [PubMed: 31669249]

Shan F, Huang Z, Xiong R, Huang QY, Li J. HIF1α-induced upregulation of KLF4 promotes migration of human vascular smooth muscle cells under hypoxia. J Cell Physiol. 2020; 235: 141–150. [PubMed: 31270801]

Sherman BT, Hao M, Qiu J, Jiao X, Baseler MW, Lane HC, Imamichi T, Chang W. DAVID: a web server for functional enrichment analysis and functional annotation of gene lists (2021 update). Nucleic Acids Res. 2022; 50: W216–w221. DOI: 10.1093/nar/gkac194 [PubMed: 35325185]

Siebel C, Lendahl U. Notch signaling in development, tissue homeostasis, and disease. Physiol Rev. 2017; 97: 1235–1294. [PubMed: 28794168]

Suzuki K, Bachiller D, Chen YP, Kamikawa M, Ogi H, Haraguchi R, Ogino Y, Minami Y, Mishina Y, Ahn K, Crenshaw EB III, et al. Regulation of outgrowth and apoptosis for the terminal appendage:external genitalia: development by concerted actions of BMP signaling. Development. 2003; 130: 6209–6220. [PubMed: 14602679]

Tate T, Xiang T, Wobker SE, Zhou M, Chen X, Kim H, Batourina E, Lin CS, Kim WY, Lu C, McKiernan JM, et al. Pparg signaling controls bladder cancer subtype and immune exclusion. Nat Commun. 2021; 12 6160 doi: 10.1038/s41467-021-26421-6 [PubMed: 34697317]

Trompette A, Ubags ND. Skin barrier immunology from early life to adulthood. Mucosal Immunol. 2023; 16: 194–207. [PubMed: 36868478]

Tsao PN, Vasconcelos M, Izvolsky KI, Qian J, Lu J, Cardoso WV. Notch signaling controls the balance of ciliated and secretory cell fates in developing airways. Development. 2009; 136: 2297–2307. DOI: 10.1242/dev.034884 [PubMed: 19502490]

Tuyl, Mv; Liu, J; Groenman, F; Ridsdale, R; Han, RNN; Venkatesh, V; Tibboel, D; Post, M. Iroquois genes influence proximo-distal morphogenesis during rat lung development. Am J Physiol Lung Cell Mol Physiol. 2006; 290: L777–L789. [PubMed: 16299054]

Tüzel E, Samli H, Kuru I, Türkmen S, Demir Y, Maralcan G, Güler C. Association of hypospadias with hypoplastic synpolydactyly and role of HOXD13 gene mutations. Urology. 2007; 70: 161–164. [PubMed: 17656229]

Udomsopagit T, Miwa A, Seki M, Shimbori E, Kadota Y, Tochio T, Sonoyama K. Intestinal microbiota transplantation reveals the role of microbiota in dietary regulation of RegIIIβ and RegIIIγ expression in mouse intestine. Biochem Biophys Res Commun. 2020; 529: 64–69. [PubMed: 32560820]

Vandenbroucke RE, Vanlaere I, Van Hauwermeiren F, Van Wonterghem E, Wilson C, Libert C. Pro-inflammatory effects of matrix metalloproteinase 7 in acute inflammation. Mucosal Immunol. 2014; 7: 579–588. [PubMed: 24129163]

Varley CL, Bacon EJ, Holder JC, Southgate J. FOXA1 and IRF-1 intermediary transcriptional regulators of PPARgamma-induced urothelial cytodifferentiation. Cell Death Differ. 2009; 16: 103–114. [PubMed: 18688264]

Vezina CM, Allgeier SH, Fritz WA, Moore RW, Strerath M, Bushman W, Peterson RE. Retinoic acid induces prostatic bud formation. Dev Dynam. 2008; 237: 1321–1333. DOI: 10.1002/dvdy.21526 [PubMed: 18393306]

Warrick JI, Walter V, Yamashita H, Chung E, Shuman L, Amponsa VO, Zheng Z, Chan W, Whitcomb TL, Yue F, Iyyanki T, et al. FOXA1, GATA3 and PPARγ cooperate to drive luminal subtype in bladder cancer: a molecular analysis of established human cell lines. Sci Rep. 2016; 6 38531 doi: 10.1038/srep38531 [PubMed: 27924948]

Weaver M, Yingling JM, Dunn NR, Bellusci S, Hogan BL. Bmp signaling regulates proximal-distal differentiation of endoderm in mouse lung development. Development. 1999; 126: 4005–4015. [PubMed: 10457010]

Xiong Z, Ren S, Chen H, Liu Y, Huang C, Zhang YL, Odera JO, Chen T, Kist R, Peters H, Garman K, et al. PAX9 regulates squamous cell differentiation and carcinogenesis in the oro-oesophageal epithelium. J Pathol. 2018; 244: 164–175. DOI: 10.1002/path.4998 [PubMed: 29055049]

Xu K, Wu X, Shapiro E, Huang H, Zhang L, Hickling D, Deng Y, Lee P, Li J, Lepor H, Grishina I. Bmp7 functions via a polarity mechanism to promote cloacal septation. PLoS One. 2012; 7 e29372 doi: 10.1371/journal.pone.0029372 [PubMed: 22253716]

Xue AG, Chan M, Gujral TS. Pan-cancer analysis of the developmental pathways reveals non-canonical wnt signaling as a driver of mesenchymal-type tumors. Transl Res. 2020; 224: 1–15. [PubMed: 32522670]

Yamaguchi TP, Bradley A, McMahon AP, Jones S. A Wnt5a pathway underlies outgrowth of multiple structures in the vertebrate embryo. Development. 1999; 126: 1211–1223. [PubMed: 10021340]

Yin C, Ye Z, Wu J, Huang C, Pan L, Ding H, Zhong L, Guo L, Zou Y, Wang X, Wang Y, et al. Elevated Wnt2 and Wnt4 activate NF-κB signaling to promote cardiac fibrosis by cooperation of Fzd4/2 and LRP6 following myocardial infarction. EBioMedicine. 2021; 74 doi: 10.1016/j.ebiom.2021.103745 [PubMed: 34911029]

Yoshida K, Kubo A, Fujita H, Yokouchi M, Ishii K, Kawasaki H, Nomura T, Shimizu H, Kouyama K, Ebihara T, Nagao K, et al. Distinct behavior of human Langerhans cells and inflammatory dendritic epidermal cells at tight junctions in patients with atopic dermatitis. J Allergy Clin Immunol. 2014; 134: 856–864. [PubMed: 25282566]

Yu Z, Liao J, Chen Y, Zou C, Zhang H, Cheng J, Liu D, Li T, Zhang Q, Li J, Yang X, et al. Single-cell transcriptomic map of the human and mouse bladders. J Am Soc Nephrol. 2019; 30 (11) 2159–2176. DOI: 10.1681/ASN.2019040335 [PubMed: 31462402]

Zenhom M, Hyder A, Kraus-Stojanowic I, Auinger A, Roeder T, Schrezenmeir J. PPARγ-dependent peptidoglycan recognition protein 3 (PGlyRP3) expression regulates proinflammatory cytokines by microbial and dietary fatty acids. Immunobiology. 2011; 216: 715–724. [PubMed: 21176858]

Europe PMC Funders Author Manuscripts

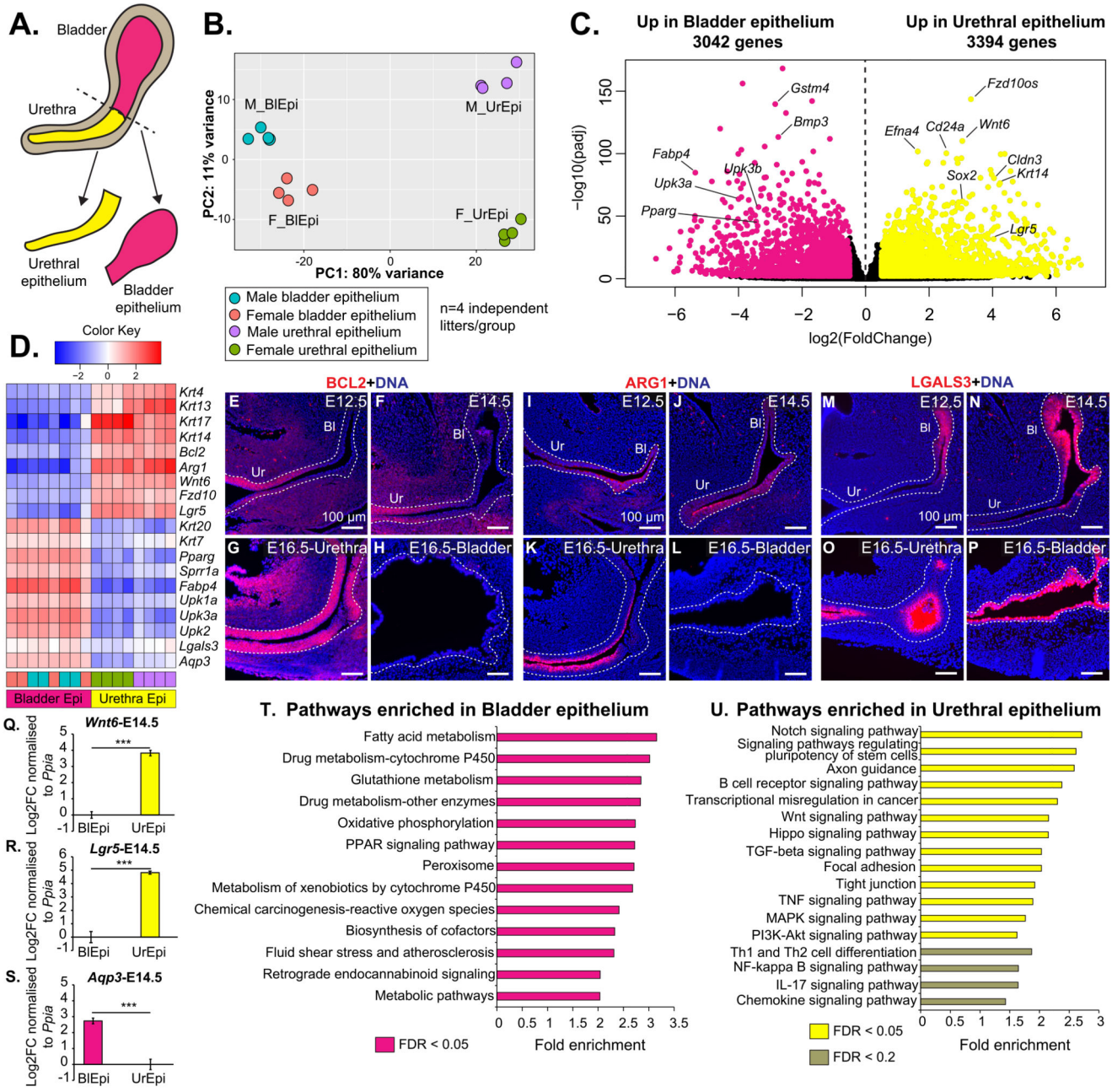

Fig. 1. Distinct epithelial compartments in the developing lower urinary tract.

(A) Schematic of epithelial layer isolation from E16.5 mouse lower urinary tracts. (B) Plot of Principal component 1 versus Principal component 2 obtained after Principal components analysis from RNA-sequencing of the bladder epithelium and urethral epithelium. (C) Volcano plot depicting differentially expressed genes which have higher expression in the bladder epithelium (magenta dots) and urethral epithelium (yellow dots). Colored dots represent genes with absolute log2 fold change ≥0.5 and adjusted p-value ≤0.01. (D) Heatmap depicting select genes that show differential expression between the E16.5 bladder and urethra epithelial compartments. Fluorescent immunostaining of (E) E12.5, (F) E14.5

Europe PMC Funders Author Manuscripts

and (G–H) E16.5 lower urinary tract sections with antibodies to BCL2 (in red). Fluorescent immunostaining of (I) E12.5, (J) E14.5 and (K–L) E16.5 lower urinary tract sections with antibodies to ARG1 (in red). Fluorescent immunostaining of (M) E12.5, (N) E14.5 and (O–P) E16.5 lower urinary tract sections with antibodies to LGALS3 (in red). Cell nuclei were stained with DAPI (in blue). Each image is representative of embryos obtained from at least n = 3 independent litters. Scale bar represents 100 μm. White dotted lines indicate the basement membrane. Quantitative RT-PCR for (Q) *Wnt6*, (R) *Lgr5* and (S) *Aqp3* transcripts in E14.5 bladder and urethral epithelium. qRT-PCR was performed on samples obtained from n = 4–5 litter independent biological replicates. Student's t-test was performed and *** represents a p-value <0.001. Top enriched KEGG pathways in (T) bladder epithelium and (U) urethral epithelium. (For interpretation of the references to color in this figure legend, the reader is referred to the Web version of this article.)

Europe PMC Funders Author Manuscripts

Europe PMC Funders Author Manuscripts

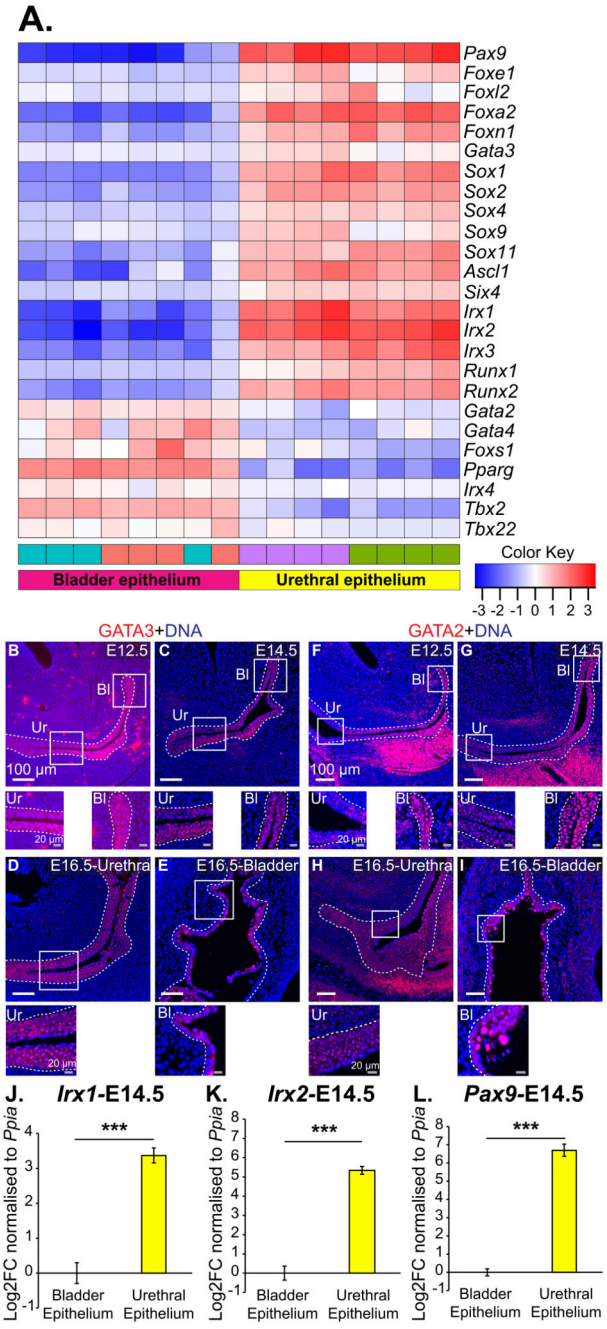

Fig. 2. Early expression of transcription factors in the bladder and urethra.

(A) Heatmap depicting select transcription factors that are differentially expressed in the epithelial compartment of the E16.5 bladder and urethra. The cut-off for differentially expressed genes was set to absolute log2 fold change ≥0.5 and adjusted p-value ≤0.01. Fluorescent immunostaining of (B) E12.5, (C) E14.5 and (D–E) E16.5 lower urinary tract sections with antibodies to GATA3 (in red). Insets show magnified regions from B-E. Fluorescent immunostaining of (F) E12.5, (G) E14.5 and (H–I) E16.5 lower urinary tract sections with antibodies to GATA2 (in red). Insets show magnified regions from F-I. Cell

nuclei were stained with DAPI (in blue). Each image is representative of embryos obtained from at least n = 3 independent litters. White scale bar represents 100 μm. Grey scale bar represents 20 μm. White dotted lines indicate the basement membrane. Quantitative RT-PCR for (J) *Irx1*, (K) *Irx2* and (L) *Pax9* transcripts in E14.5 bladder and urethral epithelium. qRT-PCR was performed on samples obtained from n = 4 litter independent biological replicates. Student's t-test was performed and asterisks indicate p value levels ***<0.001. (For interpretation of the references to color in this figure legend, the reader is referred to the Web version of this article.)

Europe PMC Funders Author Manuscripts

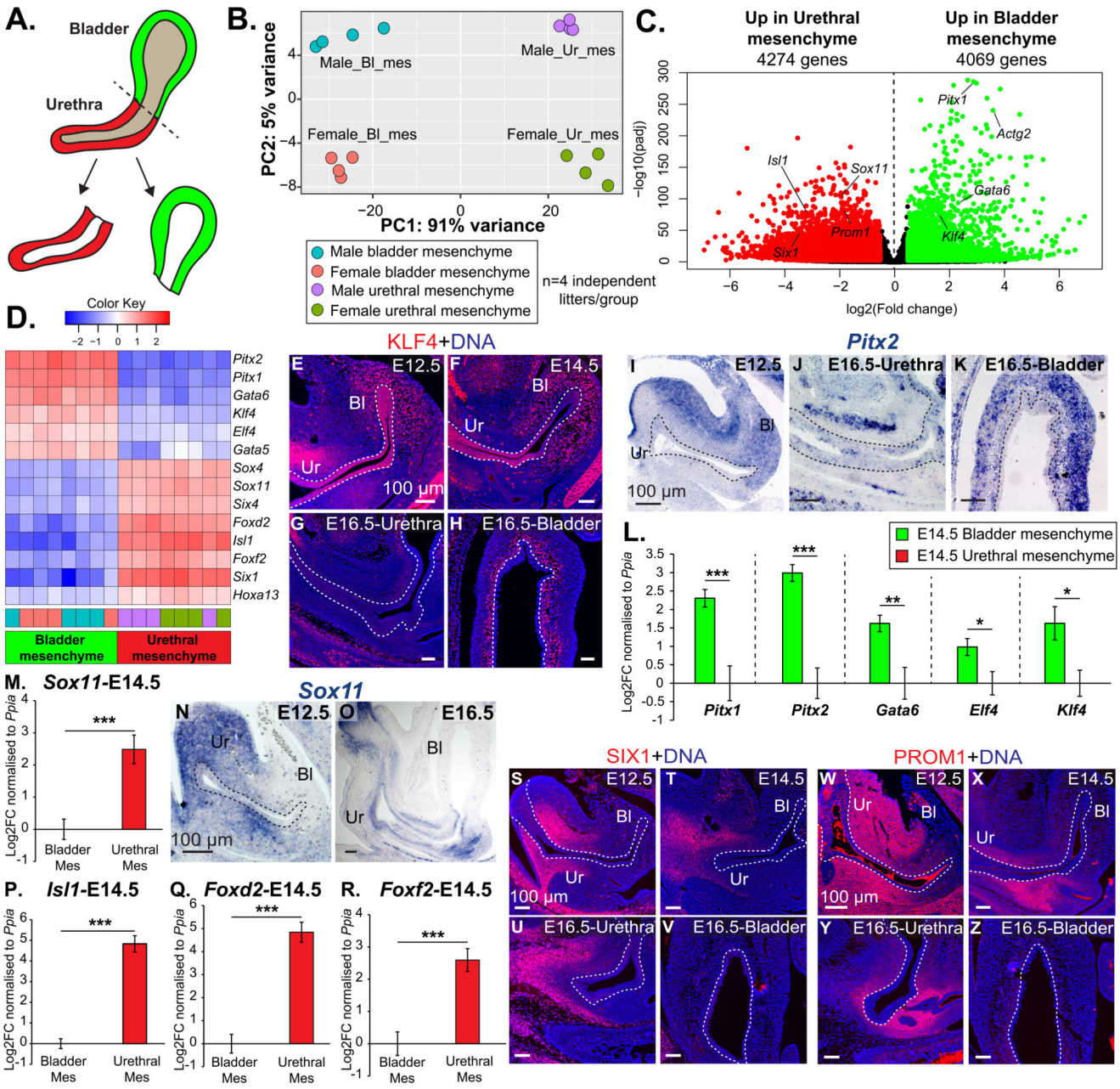

Fig. 3. Gene expression profiles of the developing bladder and urethra mesenchyme.

(A) Schematic of mesenchymal compartment isolation from E16.5 mouse lower urinary tracts. (B) Plot of Principal component 1 versus Principal component 2 obtained after Principal components analysis from RNA-sequencing of the bladder mesenchyme and urethral mesenchyme. (C) Volcano plot depicting differentially expressed genes which have higher expression in the bladder mesenchyme (green dots) and urethral mesenchyme (red dots). Colored dots represent genes with absolute log2 fold change ≥0.5 and adjusted p-value ≤0.01. (D) Heatmap depicting select transcription factors that show differential expression between the E16.5 bladder and urethra mesenchymal compartments. Fluorescent

Europe PMC Funders Author Manuscripts

immunostaining of (E) E12.5, (F) E14.5 and (G–H) E16.5 lower urinary tract sections with antibodies to KLF4 (in red). In situ hybridization for *Pitx2* mRNA was performed on embryo sections at (I) E12.5 and (J–K) E16.5. (L) Quantitative RT-PCR for *Pitx1, Pitx2, Gata6, Elf4* and *Klf4* transcripts in E14.5 bladder and urethral mesenchyme. (M) Quantitative RT-PCR *Sox11* transcripts in E14.5 bladder and urethral mesenchyme. In situ hybridization for *Sox1*1 mRNA was performed on embryo sections at (N) E12.5 and (O) E16.5. Quantitative RT-PCR for (P) *Isl1*, (Q) *Foxd2* and (R) *Foxf2* transcripts in E14.5 bladder and urethral mesenchyme. Fluorescent immunostaining of (S) E12.5, (T) E14.5 and (U–V) E16.5 lower urinary tract sections with antibodies to SIX1 (in red). Fluorescent immunostaining of (W) E12.5, (X) E14.5 and (Y–Z) E16.5 lower urinary tract sections with antibodies to PROM1 (in red). For fluorescent images, cell nuclei are labeled with DAPI (in blue). Each image is representative of embryos obtained from at least n = 3 independent litters. Scale bar represents 100 μm. White and black dotted lines indicate the basement membrane. qRT-PCR was performed on samples obtained from n = 4 litter independent biological replicates. Student's t-test was performed and asterisks indicate p value levels * <0.05, ** <0.01, ***<0.001. (For interpretation of the references to color in this figure legend, the reader is referred to the Web version of this article.)

Europe PMC Funders Author Manuscripts

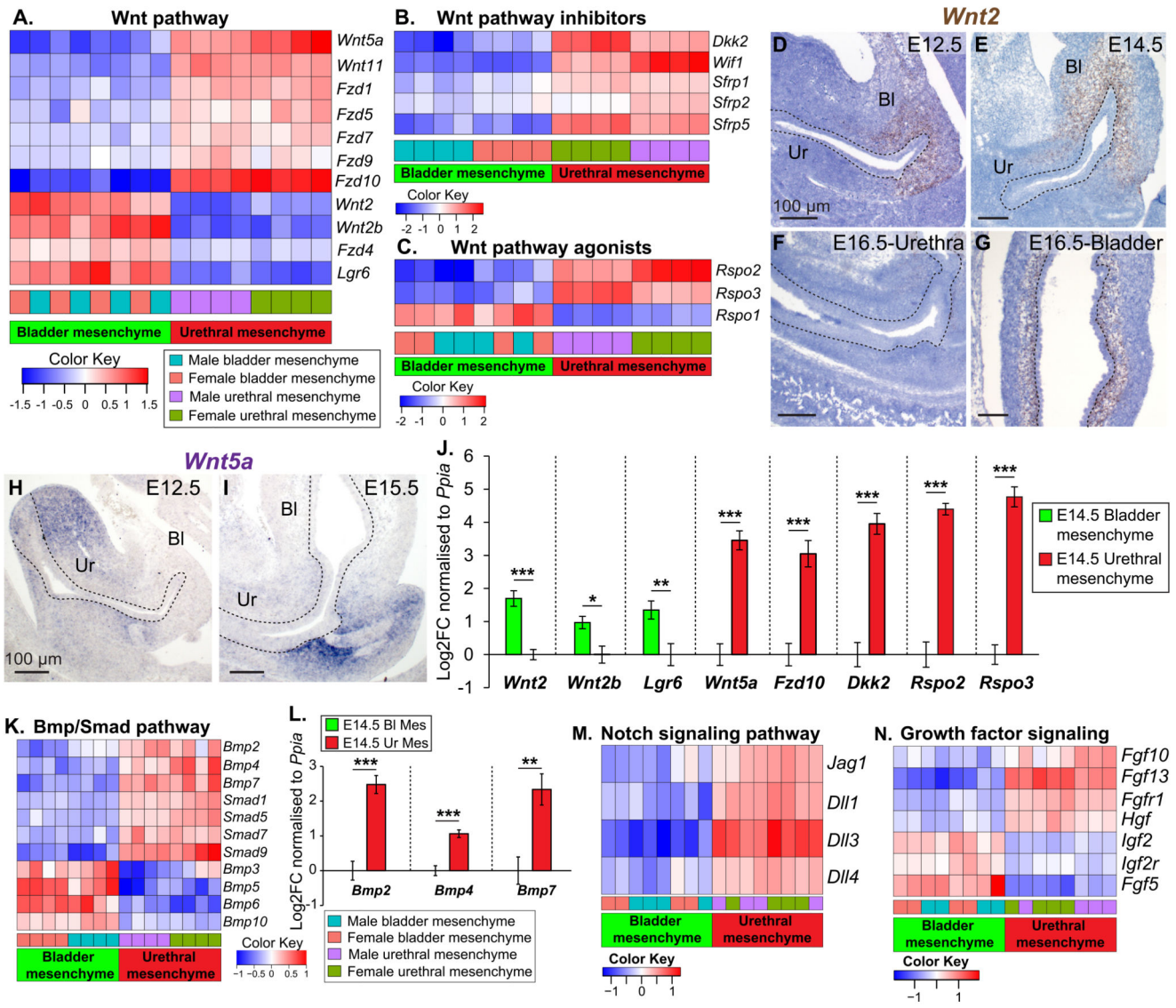

Fig. 4. Differential expression of developmental pathway genes in the urethra and bladder mesenchyme.

Heatmaps depicting select (A) Wnt ligands, receptors and co-receptors, (B) Wnt inhibitors and (C) R-spondins that show differential expression between the E16.5 bladder and urethra mesenchymal compartments (absolute log2 fold change ≥0.5 and adjusted p-value ≤0.01). Hybridization with a probe against *Wnt2* transcripts on embryo sections at (D) E12.5, (E) E14.5 and (F–G) E16.5. Sections were counterstained with hematoxylin to label nuclei. Quantitative RT-PCR for (H) *Wnt2, Wnt2b, Lgr6, Wnt5a, Fzd10, Dkk2, Rspo2* and *Rspo3* in E14.5 bladder and urethral mesenchyme. In situ hybridization for *Wnt5a* mRNA was performed on embryo sections at (I) E12.5 and (J) E15.5. (K) Heatmap of Bmp/Smad pathway genes that show differential expression between the E16.5 bladder and urethra mesenchymal compartments (absolute log2 fold change ≥0.5 and adjusted p-value ≤0.01). Quantitative RT-PCR for (L) *Bmp2, Bmp4* and *Bmp7* in E14.5 bladder and urethral mesenchyme. Heatmaps depicting differentially expressed genes in the bladder and urethral

mesenchymal compartments involved in (M) Notch signaling pathway and (N) growth factor signaling pathway. Each image is representative of embryos obtained from at least n = 3 independent litters. Scale bar represents 100 μm. Black dotted lines indicate the basement membrane. qRT-PCR was performed on samples obtained from n = 4 litter independent biological replicates. Student's t-test was performed and asterisks indicate p value levels * <0.05, ** <0.01, ***<0.001.

Europe PMC Funders Author Manuscripts

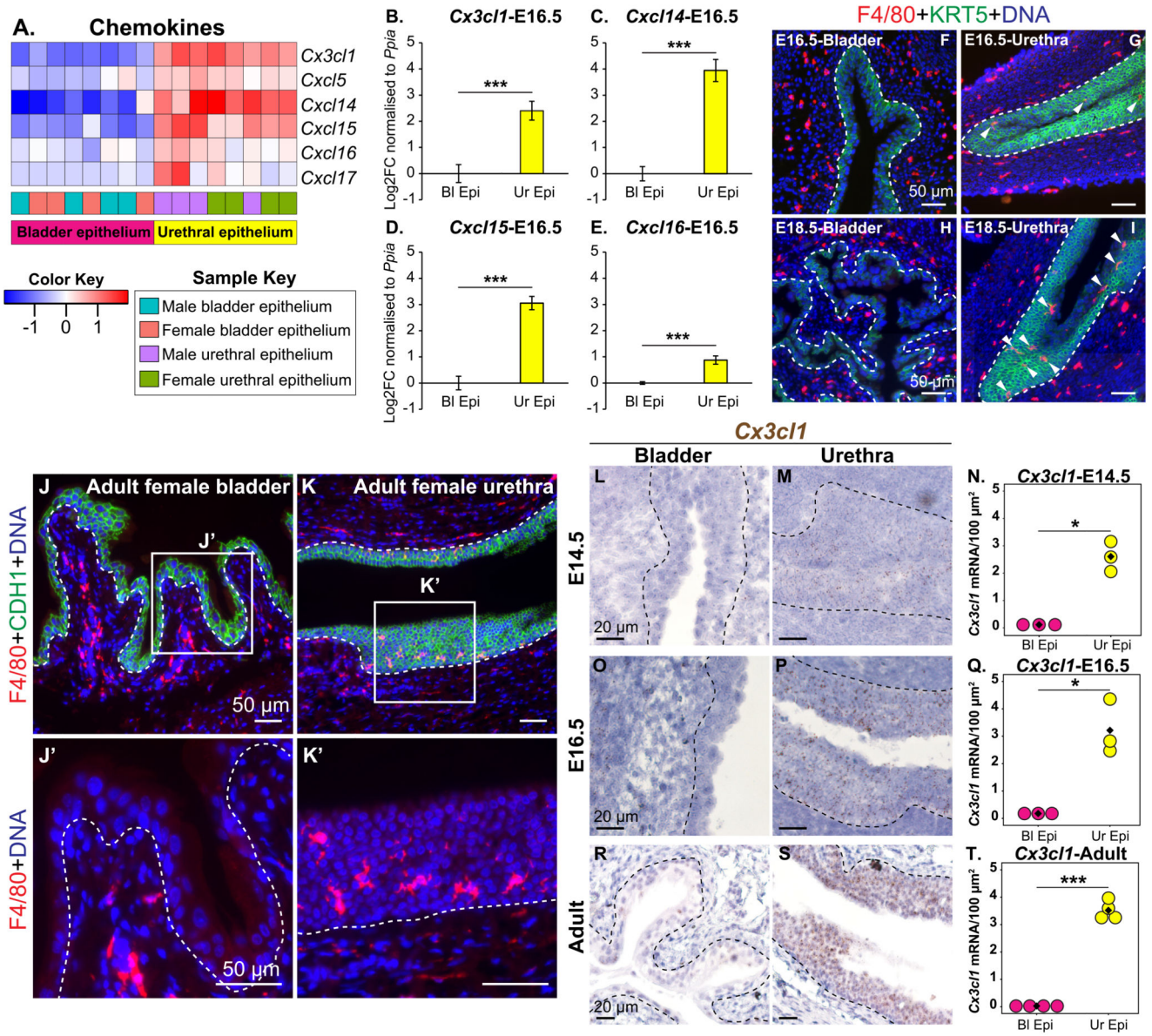

Fig. 5. Expression of chemokines and barrier function genes in the developing urethral epithelium.

(A) Heatmap depicting differentially expressed chemokine genes in the bladder and urethral epithelium. Quantitative RT-PCR for (B) *Cx3cl1*, (C) *Cxcl14*, (D) *Cxcl15* and (E) *Cxcl16* in E16.5 bladder and urethral epithelium. Fluorescent immunostaining of (F) E16.5 bladder, (G) E16.5 urethra, (H) E18.5 bladder and (I) E18.5 urethra with antibodies to F4/80 (in red) and KRT5 (in green). Cell nuclei are labeled with DAPI (in blue). Fluorescent immunostaining of (J) adult female mouse bladder and (K) adult female mouse urethra with antibodies to F4/80 (in red) and CDH1 (in green). Cell nuclei are labeled with DAPI. (J′) and (K′) indicate magnified regions from J and K respectively with F4/80 and DAPI labeling displayed. Hybridization with a probe against *Cx3cl1* transcripts on tissue sections from (L–N) E14.5, (O–Q) E16.5 and (R–T) adult stages. Images show labeling for *Cx3cl1*

Europe PMC Funders Author Manuscripts

transcripts in bladder and urethral epithelium and graphs indicate quantification of individual transcripts/100 μm^2 area. White scale bar represents 50 μm. Black scale bar represents 20 μm. White and black dotted lines indicate the basement membrane. White arrowheads indicate epithelial-associated macrophages. Each image is representative of at least n = 3 biological replicates. Welch's *t*-test was performed for *Cx3cl1* quantification and asterisks indicate p value levels * <0.05, **<0.01, ***<0.001. (For interpretation of the references to color in this figure legend, the reader is referred to the Web version of this article.)

Europe PMC Funders Author Manuscripts

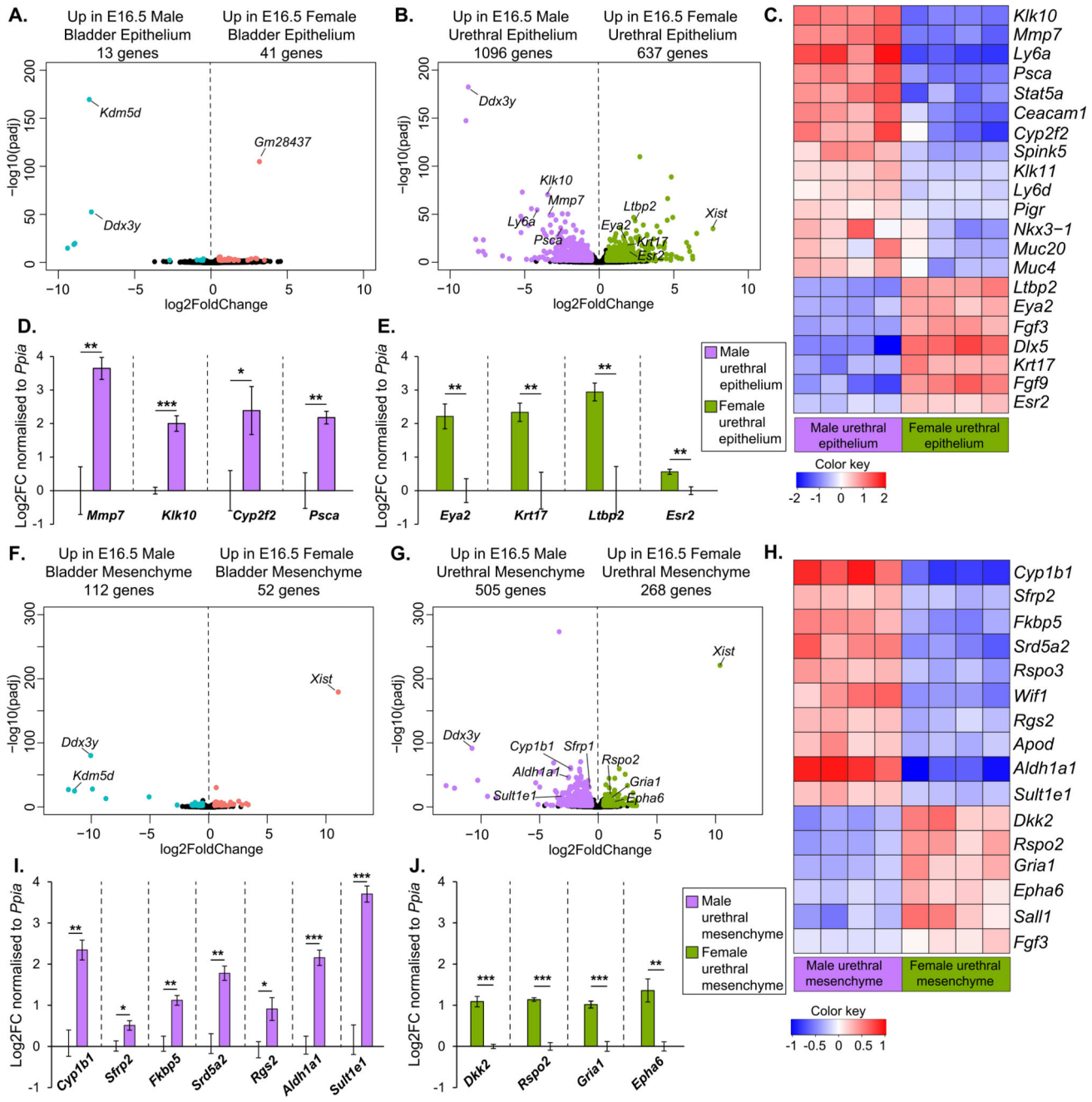

Fig. 6. Sex-specific differences in the developing lower urinary tract.

(A) Volcano plot depicting differentially expressed genes which have higher expression in the male bladder epithelium (cyan dots) and female bladder epithelium (red dots). (B) Volcano plot depicting differentially expressed genes which have higher expression in the male urethral epithelium (purple dots) and female urethral epithelium (green dots). Colored dots represent genes with absolute log2 fold change ≥0.5 and adjusted p-value ≤0.01. (C) Heatmap depicting select genes that show differential expression between the E16.5 male and female urethral epithelial compartments. (D) Quantitative RT-PCR for genes enriched

Europe PMC Funders Author Manuscripts

in E16.5 male urethral epithelium. (E) Quantitative RT-PCR for genes enriched in E16.5 female urethral epithelium. (F) Volcano plot depicting differentially expressed genes which have higher expression in the male bladder mesenchyme (cyan dots) and female bladder mesenchyme (red dots). (G) Volcano plot depicting differentially expressed genes which have higher expression in the male urethral mesenchyme (purple dots) and female urethral mesenchyme (green dots). Colored dots represent genes with absolute log2 fold change ≥0.5 and adjusted p-value ≤0.01. (H) Heatmap depicting select genes that show differential expression between the E16.5 male and female urethral mesenchymal compartments. (I) Quantitative RT-PCR for genes enriched in E16.5 male urethral mesenchyme. (J) Quantitative RT-PCR for genes enriched in E16.5 female urethral mesenchyme. qRT-PCR was performed on samples obtained from n = 4 litter independent biological replicates. Student's t-test was performed and asterisks indicate p value levels * <0.05, ** <0.01, ***<0.001. (For interpretation of the references to color in this figure legend, the reader is referred to the Web version of this article.)

Europe PMC Funders Author Manuscripts